UNIVERSITY OF OKLAHOMA

GRADUATE COLLEGE

EXAMINING LAKE-EFFECT CHANGES ACROSS THE GREAT LAKES UTILIZING DYNAMICALLY DOWNSCALED CLIMATE SIMULATIONS

A THESIS

SUBMITTED TO THE GRADUATE FACULTY

in partial fulfillment of the requirements for the

Degree of

MASTER OF SCIENCE

By

SHAUN LAURINAITIS

Norman, Oklahoma

2025

Downloaded from SHAREOK. Persistent Handle URL: https://hdl.handle.net/11244/341531

EXAMINING LAKE-EFFECT CHANGES ACROSS THE GREAT LAKES
UTILIZING DYNAMICALLY DOWNSCALED CLIMATE SIMULATIONS

A THESIS APPROVED FOR THE
SCHOOL OF METEOROLOGY

BY THE COMMITTEE CONSISTING OF

Dr. Zachary Lebo (Chair)

Dr. Jason Furtado

Dr. Steven Cavallo

© Copyright by SHAUN LAURINAITIS 2025
All Rights Reserved.

Acknowledgments

The author would like to thank Dr. Zachary Lebo for all of his advising and guidance to get to this point, as well as allowing the author to work on a project in their field of interest. They would also like to thank Dr. Victor Gensini for supplying the downscaled model simulation dataset, Dr. Steven Cavallo for ideas and guidance on analysis techniques, and Dr. Jason Furtado for assistance and guidance on statistical analysis techniques.

List Of Figures

1.1 Conceptual model of the electrical structure within lake-effect snow bands in a vertical cross-section. The legend shows the meaning of symbols and distances along the ground are relative to the lake shore. The electric charge is indicated on ice crystal, snow, and graupel hydrometeors to show regions of electric potential. Figure reproduced from Figure 7 of Steiger et al. (2024) with permission from author. 8
1.2 Seasonal Snowfall Departures in the Northeast for the last 6 winter seasons from October 1st to April 30th. Data are reproduced from the Northeast Regional Climate Center (Northeast Regional Climate Center 2025). 10

3.1 Central plot depicts the study domain, including locations of the sites prone to lake effect snow used in this study. Surrounding plots compare the snowfall amounts corresponding to various percentiles of 6-hourly snowfall accumulations at each site in the historical (blue) and EOC (red) periods. 21
3.2 Spatial distribution of relative changes in the seasonal average snowfall accumulation between the EOC and historical periods for (a) SON, (b) DJF, and (c) MAM (units: %). Hatching signifies significant changes at the 99% confidence level with 10000 iterations using the bootstrapping approach summarized in the Data and Methods Chapter 2. 22
3.3 Spatial distribution of the changes (EOC minus historical) in the number of occurrences of the a) favorable temperature criterion, b) favorable instability criterion, c) favorable 850 mb wind criterion, d) mean favorable 900-700 mb wind criterion, and e) all favorable criteria being met as well as the change in average 10-m convergence during favorable lake-effect times in panel f. Panel g shows a monthly occurrence histogram of times when all conditions are met with the 10 °C instability criteria for the EOC and historical periods in red and blue, respectively. 26
3.4 Spatial distribution of changes in the top 10, 5, and 1% 6-hourly snowfall accumulations during favorable lake-effect conditions with the 10 °C instability criteria (EOC - Historical). The change in the snowfall accumulation corresponding to each percentile is shown in mm per 6 hours. 27

3.5 Changes in the average 6-hourly snowfall accumulation during all snowfall periods (left) and during favorable lake-effect conditions with the 10 °C instability criterion snowfalls (right) between periods (EOC - Historical). Hatching signifies significant changes at the 99% confidence level using the bootstrapping approach summarized in the Data and Methods Chapter 2. 29
3.6 Changes in (a) the occurrences of and (b) the average event total snowfall for classified favorable 10 °C instability lake-effect events. The distribution of the average event total snowfalls over the domain in each winter season as well as the number of classified events per season (diamonds) is shown for both (c) the historical and (d) EOC periods as violin plots. A season year is defined as the year of the JFM months in a given winter season, where a winter season contains events from October to May. The distribution of average event total snowfalls over each entire period is shown in panel (e) as violin plot. White dashed lines in the distributions show the quartiles of each distribution. The distribution of the durations of the classified lake-effect events for each period is shown in panel (f), with the resulting p-value from a 2-sample Kolmogorov-Smirnov test for significant changes in the distributions in the bottom right of the panel. 31
3.7 Same as Figure 3.3 but for the favorable 13 °C lake-effect snow criteria. Panels a, c, and d are the same as in Figure 3.3. 34
3.8 Same as Figure 3.4 but for favorable 13 °C lake-effect snow criteria. . . 36
3.9 Same as Figure 3.5 but for snowfalls during favorable lake-effect conditions with the 13 °C instability criteria. 36
3.10 Same as Figure 3.6 but for classified favorable 13 °C instability lake-effect events. 39
3.11 Season total snowfall time series during the historical period for each site of interest from all snowfall (solid line, circle marks), snowfall during favorable 10 °C instability criteria times (dashed line, square marks), and snowfall during favorable 13 °C instability criteria times (dotted line, triangle marks). 41
3.12 Season total snowfall time series during the EOC period for each site of interest from all snowfall (solid line, circle marks), snowfall during favorable 10 °C instability times (dashed line, square marks), and snowfall during favorable 13 °C instability times (dotted line, triangle marks). . 43

4.1 Changes in the monthly average temperature differential between 2 meters and 850 mb over the Great Lakes for each month during the cold season. 46

4.2 Composite soundings for favorable 10 °C instability snowfall times where at least 0.1 in (2.54 mm) of 6-hourly snowfall was recorded at each site of interest. Red and green solid (dashed) lines show the historical (EOC) temperature and dew point profile, respectively. Black (red) wind barbs show the Historical (EOC) wind profile. Sites off Lake Ontario are shown in panels a and b, off Lake Erie shown in panels c and d, off Lake Superior in panels e and f, off Lake Huron in panels g and h, and off Lake Michigan in panels i and j. 48
4.3 Composite soundings for favorable 13 °C instability snowfall times where at least 0.1 in (2.54 mm) of 6-hourly snowfall was recorded at each site of interest. Red and green solid (dashed) lines show the historical (EOC) temperature and dew point profile, respectively. Black (red) wind barbs show the Historical (EOC) wind profile. Sites off Lake Ontario are shown in panels a and b, off Lake Erie shown in panels c and d, off Lake Superior in panels e and f, off Lake Huron in panels g and h, and off Lake Michigan in panels i and j. 50
4.4 Map of the domain highlighting the sites of interest examined in this study as well as the locations of their upwind composite sounding sites shown by the square markers with colors corresponding to each respective downwind site. 52
4.5 Same as Figure 4.2 but for points 50 km upstream of each site of interest. 52
4.6 Same as Figure 4.3 but for points 50 km upstream of each site of interest. 54
4.7 Changes between periods (EOC - Historical) in the average echo top height in meters (left) and the relative change in the average maximum updraft speed in percent (right) during favorable 10 °C instability times. Hatching signifies significant changes at the 99% confidence level using the bootstrapping approach summarized in the Data and Methods Chapter 2. 56
4.8 Changes between periods (EOC - Historical) in the average echo top height in meters (left) and the relative change in the average maximum updraft speed in percent (right) during favorable 13 °C instability times. Hatching signifies significant changes at the 99% confidence level using the bootstrapping approach summarized in the Data and Methods Chapter 2. 57

5.1 Grayscaled composite reflectivity imagery designated as (a) pure lake-effect precipitation, (b) a hybrid of lake-effect and non-lake-effect precipitation, (c) non-lake-effect precipitation. 66
5.2 Grayscaled composite reflectivity imagery from a random favorable 10 °C instability lake-effect snow time. In this instance, a Type I long-lake-axis-parallel (LLAP) lake-effect snow band is simulated over eastern Lake Ontario. 68

5.3 Grayscaled composite reflectivity imagery from a random favorable 10 °C instability lake-effect snow time. In this instance, a Type II short lake-axis lake-effect snow band is simulated over Lake Superior and Lake Huron. 69
5.4 Grayscaled composite reflectivity imagery from a random favorable 10 °C instability lake-effect snow time. In this instance, a Type III hybrid lake-effect snow band is simulated over Lake Superior downwind over Lake Huron reaching to northern Lake Ontario. 70
5.5 Grayscaled composite reflectivity imagery from a random favorable 10 °C instability lake-effect snow time. In this instance, a Type IV near-shore wind parallel lake-effect snow band is simulated over eastern Lake Superior. 71
5.6 Grayscaled composite reflectivity imagery from a random favorable 10 °C instability lake-effect snow time. In this instance, a Type V mesovortex lake-effect snow band is simulated over southern Lake Michigan. 72

Abstract

The Laurentian Great Lakes are home to unique mesoscale lake-effect snow bands that often form in the boreal cold season under specific conditions and are notorious for extreme whiteout conditions, high snowfall accumulations, and localized impacts to travel and economics across the region. The electrification of lake-effect snow bands via locally intense convection can produce thundersnow, creating potential hazards for infrastructure and those outside. These events develop under temperature, wind speed and shear, and instability conditions, which are expected to change in a warming climate. Thus, it is important to understand how climate change could impact lake-effect precipitation. General circulation models (GCMs), which are the primary tools used to study climate change and its impacts on weather systems, are currently too coarse to resolve mesoscale processes, such as lake-effect precipitation, which has posed a challenge for prior studies. Downscaling of these GCM simulations is needed to more accurately resolve the relevant process.

This study examines new data from a high-resolution dynamically downscaled GCM over the contiguous United States. These new data provide a resolution sufficient to explicitly resolve convective processes, such as those pertinent for lake-effect precipitation, and can be used to quantify spatial and temporal changes in lake-effect snow processes. Two 15-year periods of data are examined, consisting of historical (1990-2005) and end-of-century (2085-2100) conditions under the Representative Concentration Pathway (RCP) 8.5 climate scenario. It is found that snowfall from lake-effect snow events is expected to retain their intensity or even increase in intensity over certain parts of the region. The most intense lake-effect snowfalls are expected to become even more intense, especially off portions of Lake Superior and Lake Huron. This increase in intensity is due to increasing lake surface air temperatures and therefore lower-level instability for lake-effect bands to utilize, although the temperatures remain cold enough for precipitation to remain as snow. Owing to the increase in temperature,

lake-effect snowfall occurrences are also more constrained to the core winter season and are expected to decrease by the end of the century. Likewise, continuous snowfall events are expected to produce more snowfall on average while becoming less common and slightly longer in duration. With increased low-level instability lake-effect snow bands are expected to become deeper and contain stronger updrafts, perhaps increasing the number of lake-effect electrification and thundersnow occurrences in a warming world.

Table of Contents

Acknowledgments **iv**

List Of Figures **v**

Abstract **ix**

1 Introduction **1**
1.1 Lake-Effect Band Types and Impacts 3
1.2 Lake-Effect Lightning 5
1.3 Observed Trends in Lake-Effect Snow and Ice Cover 8
1.4 Future Trends in Lake-Effect Snow 12

2 Data and Methods **14**
2.1 Lake-Effect Criteria Selection 15
2.1.1 Classifying Lake-Effect Snow Events 17
2.2 Statistical Analysis Methods 17

3 Lake-Effect Snowfall **19**
3.1 Overall Changes in Snowfall 19
3.2 Changes in Lake-Effect Snowfall 23
3.3 Changes in Classified Lake-Effect Snow Events 29
3.4 Sensitivity to Instability Thresholds 32
3.5 Site Snowfall Comparisons 40

4 Lake-Effect Properties **44**
4.1 Changes in Monthly Average Instability 44
4.2 Changes in Lake-Effect Environments 47
4.3 Changes in Electrification Properties of Lake-Effect Snow 54

5 Summary and Conclusions **58**
5.1 Summary 58
5.2 Future Steps and Analysis 64

Reference List **72**

Chapter 1

Introduction

The Laurentian Great Lakes are a system of freshwater lakes that span part of the border between the United States of America and Canada, and together with the St. Lawrence River form a large watershed system (Environmental Protection Agency 2025). These lakes contain roughly 84% of North America's surface fresh water and 21% of the entire world's surface fresh water, with a few of the lakes being some of the largest freshwater lakes in the world (Environmental Protection Agency 2025). These large lakes and their position within the northern part of the North American continent provide a unique setting for the phenomenon of lake-effect and lake-enhanced precipitation. This type of precipitation occurs when sufficiently cold air moves over the relatively warmer waters of the lakes, creating a low-level instability as well as a thermal and moisture flux from the lake surface upward into the air above it. This process creates convective instability and convective precipitation within air masses that are usually polar or arctic in nature and are stable. These lake-effect precipitation events occur most commonly within the fall and winter months and can produce localized rains or snowfalls when surface temperatures are near or below freezing. The main season for lake-effect snow is from November to March when temperatures are often cold enough for snowfall and lake temperatures are significantly warmer than mid-level temperatures. Some early season events can occur before this in September and October and late season events from late March to as late as May, but are usually weaker and produce rainfall due to warmer temperatures and less low-level instability.

In the late 20th century, multiple different environmental parameters and patterns were concluded to be significant in the formation and predictability of lake-effect precipitation. These were especially utilized in forecasting for lake-effect snow, which is commonly more disruptive than lake-effect rain. The following forecast variables were discussed by Niziol et al. (1995) as being important in the forecasting of lake-effect snow across eastern North America. First, a large temperature differential (ΔT) between the lake and 850 mb is needed to provide ample instability for lake-effect snow bands to form. A widely used threshold operationally for this value in lake-effect precipitation forecasting is for a ΔT of 13 °C, or near a dry adiabatic lapse rate for pure lake-effect snow. The height and strength of the inversion found within the profile of a cold air mass is also important in diagnosing the potential for the depth of any lake-effect bands. As lake-effect is naturally a shallow process due to the shallow nature of cold air masses, the winds in the lower levels are crucial for the direction, evolution, and type of any formed lake-effect bands. This steering level is operationally used at the 850 mb or 700 mb level, with the entire "steering" layer for lake-effect storms often defined as the winds from the surface to 700 mb (Niziol 1987). Within this steering layer, directional wind shear below 30° is needed for organized lake-effect activity to form and persist. Too much wind shear serves to disrupt the shallow updrafts present in these systems (Niziol 1987). Low-level convergence, whether contributed by frictional differences between land and water or by mesoscale phenomena, such as lake and land breezes, is needed for and contributes to band initiation, progression, and intensity. Finally, background synoptic lift or the lack of it can enhance lake-effect convection or serve to destroy it and prevent it from forming.

1.1 Lake-Effect Band Types and Impacts

There also exists different lake-effect band types that are dependent on these conditions, such as steering layer wind direction and speed, as well as the length of space or fetch that air parcels spend over the warm lake waters. The lake-effect band types are described well by Niziol et al. (1995) and all come with different characteristics and impacts:

- **Type I** lake-effect bands are well-organized long-lake-axis-parallel (LLAP) bands that are parallel to the longer lake shores and singular. These bands can be 20-50 km wide and 50-200 km long, and are responsible for many high-impact lake-effect snow events as they contain some of the heaviest snowfalls out of all bands (Moore and Orville 1990).

- **Type II** lake-effect bands occur over the shorter axes of the lakes and are usually perpendicular to the shore and numerous in number. Anywhere from 5-20 km wide and 20-50 km long, these bands are often less intense than Type I bands and commonly affect wider areas.

- **Type III** bands are a hybrid of Type I and II bands and are characterized by long single bands of convection that stem from upstream connections with other lakes. These bands often form as a Type I band over a certain lake, such as Lake Huron, and then propagate over a landmass, such as the province of Ontario, Canada, before then reforming or intensifying as it crosses Lake Ontario or Lake Erie. With the increased moisture and convergence from upstream connections these bands can reach locations far inland from the Great Lakes, such as the Appalachians or eastern New York and can produce significant snowfall.

- **Type IV** lake-effect bands are wind parallel bands that form with weak background winds. They often occur with Arctic high pressures and are highly dependent on convergence zones near the shores of the lakes such as land breezes in these cold patterns. These bands often do not move away from these near-shore convergence zones and produce "fluffier" snow due to higher snow to water ratios (Passarelli and Braham 1981).

- **Type V** lake-effect bands form in lake breeze convergence zones in response to bowl-shaped shoreline configurations and are also called mesoscale vortices. These bands often occur more over the Upper Great Lakes (Lake Superior, Lake Michigan, and Lake Huron) and are shallow under stable conditions (Forbes and Merritt 1984; Niziol et al. 1995).

Lake-effect snow events contain multiple different hazards that impact communities, travel, and economics in the region. These snow bands often are long and narrow, as mentioned previously, and can have snowfall rates of up to 3-4 inches per hour or more. These intense snowfall rates, often coexistent with near white-out conditions, can overwhelm local maintenance crews attempting to keep roads clear for travel. The low visibility present in the heart of these lake-effect snow bands can also lead to hazardous driving conditions and even accidents, with many cases of multi-vehicle pileups on major roads from these events as well as vehicles and their commuters stuck in the heavy accumulating snow. The October 12-13, 2006, lake-effect snow event in Buffalo, NY for example was a rare early season lake-effect snow event that led to the power loss of nearly 1 million residents in the area. This storm produced around $150 million in damage and disruption costs and led to the closure of around 100 miles of U.S. Interstate 90 (National Weather Service 2006). Other high-end lake-effect snow events have also been shown to be crippling or even deadly. A compound event of two

extreme lake-effect snow events within a week paralyzed the metro area of Buffalo, NY, in November 2014. The first event led to 13 fatalities and was responsible for 1000's of stranded motorists with peak snowfall rates of near 6 inches per hour. The second event occurred only a day later, with both events dropping nearly 9 feet of snow in parts of the metro (National Weather Service 2014a,b). More recently, the December 23-27 lake-effect blizzard in 2022 brought wind chills of -10 to -20 °F and 37 hours of blizzard conditions to the Buffalo, NY, metro. Hundreds of cars were stranded and multiple fatalities reported, with snowfall totals over 50 inches off both Lake Erie and Lake Ontario by the end of the near week-long event (National Weather Service 2022).

1.2 Lake-Effect Lightning

Wintertime lightning is another hazard that is present within lake-effect snowstorms. Locally intense convection and hydrometeors including ice crystals, graupel, and the presence of supercooled water assist in the induction of charge separation within lake-effect bands. These charge regions can then produce lightning, both intra-cloud (IC) and cloud-to-ground (CG) (See Figure 1.1). These lightning occurrences create thundersnow, a phenomena in which lightning and thunder are observed while snow is precipitating. Some of these cloud-to-ground bolts of lightning have been proven to strike buildings, trees, and tall objects, potentially causing damage. Moore and Orville (1990) were some of the first to present their research on this phenomenon and found nearly 900 CG flashes during a two-day lake-effect event in September 1983. They also found that lightning events had higher inversion bases and stronger inversion strengths than those without. Steiger et al. (2009) found that lake-effect lightning was most common between September and December when the lake waters were still significantly warmer than the above air masses. 27% of lightning events were found to occur

between January and March. Most thundersnow cases occurred in Type I lake-effect bands, and nearly all lightning events were associated with lake-induced equilibrium levels greater than 3.6 km above ground level (Steiger et al. 2009).

Letcher and Steiger (2010) performed a climatology of lake-effect lightning over the Great Lakes and found that Lake Erie and Lake Ontario produced the highest number of thundersnow events, with Lake Ontario having more lightning than Lake Erie. Over the Upper Great Lakes (Lake Superior, Lake Michigan, and Lake Huron) it was found that the majority of lake-effect lightning events were associated with early-season rain and mixed-phase events, while Lake Erie and Lake Ontario displayed mainly thundersnow events. During the Ontario Winter Lake-effect Systems (OWLeS) Project, all observed lightning occurred over land, a change from the climatology discussed previously by Letcher and Steiger (2010) where many flashes occurred over lake waters. Many of these lightning flashes propagated near tall objects, with 43% of the lightning in a single Intensive Observation Period (IOP) occurring within 300 m of a tall, manmade object and thus is speculated by the authors to possibly have been initiated by these objects (Steiger et al. 2018). Many tall objects such as wind turbines were recently built to the east of Lake Ontario, which is theorized to have changed the lake-effect lightning climatology in the region (Steiger et al. 2018). Finally, a recent field campaign to the east of Lake Ontario recorded 246 flashes associated with frozen precipitation during the project using Lightning Mapping Array (LMA) data. Similarly to Steiger et al. (2018), roughly 33% of these recorded flashes occurred within 300 m of tall towers, suggesting that the presence and construction of these man-made objects may be contributing to CG lightning during lake-effect snow events and may pose a hazard to infrastructure as well as those outside during these events (Steiger et al. 2024). Given all the previously discussed socioeconomic impacts of lake-effect snow

events, understanding current and future trends in these systems and their potential impacts is of great importance.

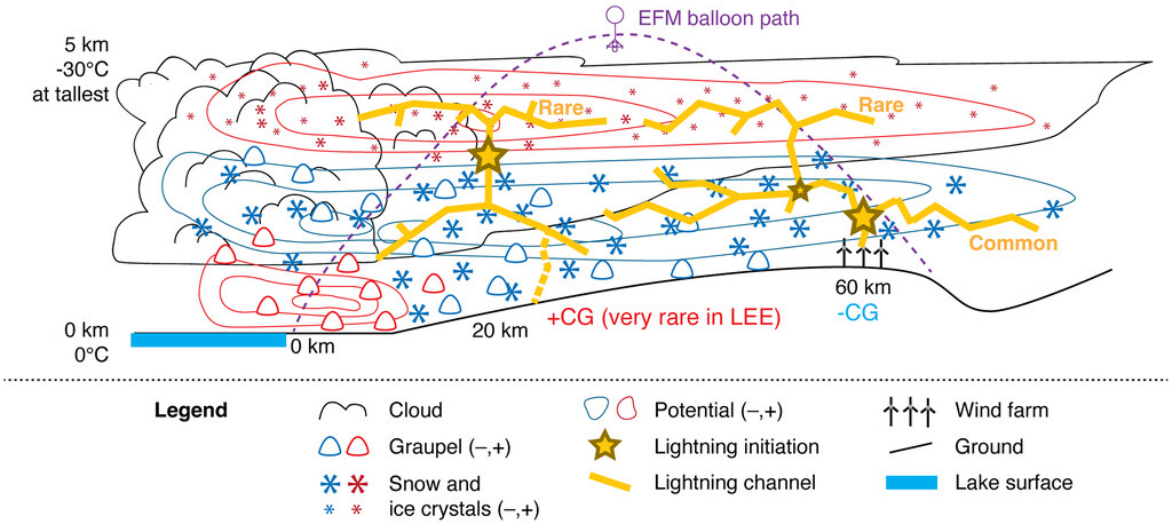

Figure 1.1: Conceptual model of the electrical structure within lake-effect snow bands in a vertical cross-section. The legend shows the meaning of symbols and distances along the ground are relative to the lake shore. The electric charge is indicated on ice crystal, snow, and graupel hydrometeors to show regions of electric potential. Figure reproduced from Figure 7 of Steiger et al. (2024) with permission from author.

1.3 Observed Trends in Lake-Effect Snow and Ice Cover

Previous research has shown decreasing snowfall trends in the Great Lakes region attributed to climate change. Ashley et al. (2020) found that the greatest reduction in the occurrence of snow has occurred over the northern Great Lakes, while Baijnath-Rodino et al. (2018) identified negative snowfall trends during much of the cold season (November to March) along the Canadian shores of Lake Superior and Lake Huron. It has been shown that snowfall contributed by the Great Lakes has experienced a trend reversal and is decreasing downwind of Lake Michigan (Bard and Kristovich 2012). Suriano and Leathers (2017) identified 7 lake-effect synoptic types or patterns across the eastern Great Lakes and found that 6 out of 7 of them showed increased frequencies from 1950-1979, with the majority of these types/patterns exhibiting a decrease in

frequency from 1980-2009 along with their associated snowfall amounts. Similarly, Suriano (2019) identified four atmospheric patterns as lake-effect synoptic types and noted that each exhibited decreasing temperatures and surface pressures, as well as increasing boundary layer instability and zonal flow from 1950-1979 with observed snowfall increases. These types then remained relatively unchanged or decreased in frequency along with their associated snowfall amounts from 1980-2009. Across central New York, downwind of Lake Ontario, Hartnett et al. (2014) found negative snowfall trends over the past 41 years based on observations. Many areas within the Great Lakes have also experienced negative snowfall departures compared to climatology over the past decade, as shown by Figure 1.2. Here, substantial and consistent negative seasonal snowfall anomalies can be seen in prominent lake-effect snow belts, such as the areas south and east of both Lake Ontario and Lake Erie (Northeast Regional Climate Center 2025).

In contrast, Burnett et al. (2003) found significant upward trends in cold-season snowfall for 11 out of 15 lake-effect sites studied. Non-lake-effect stations saw no significant trends, and oxygen isotope data from the eastern Finger Lakes revealed a positive trend in lake-effect snow as well. Kunkel et al. (2009) utilized trend analysis for suitable long-term observation stations in lake-effect snow belts and found an upward trend in snowfall and liquid equivalent snow for sites off Lake Superior and Lake Michigan. For Lake Ontario and Lake Erie, no distinct trend was present, as the trends at these stations depended on the time period of analysis. Other recent studies have examined trends in lake and river ice cover across the entire Northern Hemisphere, with Magnuson et al. (2000) observing later freezing dates and earlier ice breakup dates in many lakes and rivers. With shorter durations of ice cover on the lakes, open waters

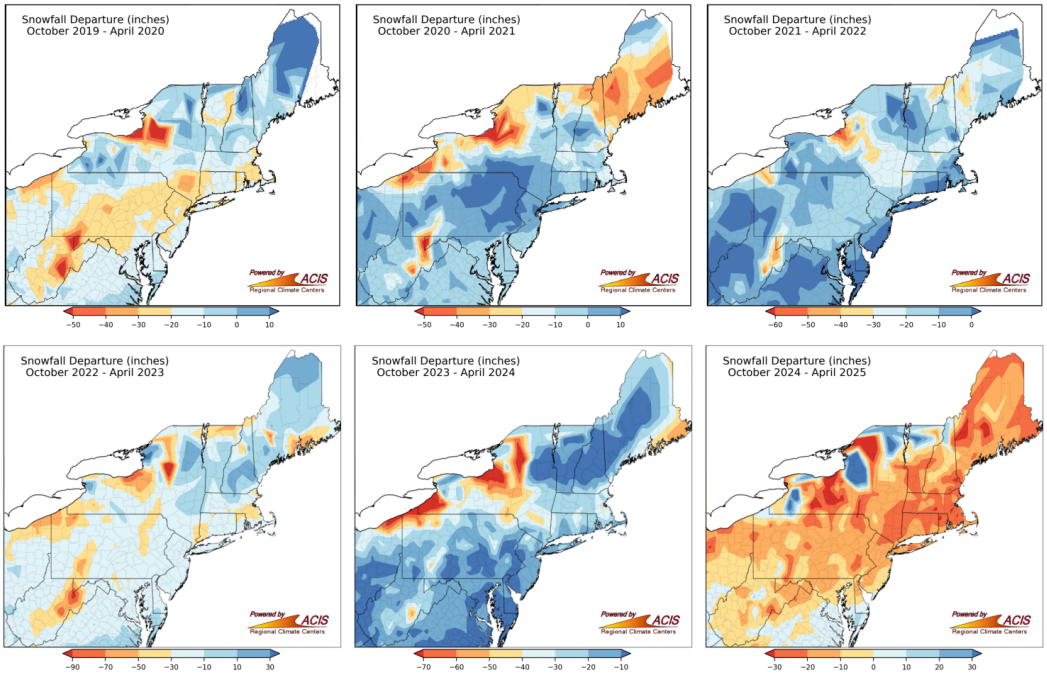

Figure 1.2: Seasonal Snowfall Departures in the Northeast for the last 6 winter seasons from October 1st to April 30th. Data are reproduced from the Northeast Regional Climate Center (Northeast Regional Climate Center 2025).

conducive for lake-effect snow will be present for longer, potentially increasing the season for lake-effect snow and intensifying it. The interannual variability in these dates was also found to have increased since 1950. Focusing on ice cover in the Great Lakes, some have found significant downward trends in ice cover on all of the lakes, with the largest changes occurring on Lake Ontario, Lake Michigan, and Lake Superior (Wang et al. 2012). Assel et al. (2003) examined the annual maximum ice cover (AMIC) over each of the Great Lakes and 4-year running means of this value showed stark decreases in the more recent years of the study, especially over Lake Superior. Mason et al. (2016) also found consistent linear declines in seasonal ice cover duration in 11 out of 17 defined sub-basins across the Great Lakes. Using long-term trends in modeled lake surface temperatures (LSTs) and ice cover, Cannon et al. (2024) showed significant warming in LSTs in all seasons with the strongest in the winter and spring seasons,

and within Lake Ontario and Lake Superior. Negative changes in ice characteristics, such as ice thickness and AMIC, were greatest over northern portions of each lake, with changes in ice cover being the smallest over Lake Ontario and Lake Michigan.

These trends in ice cover are extremely important to the creation, maintenance, and intensity of lake-effect snow. Vavrus et al. (2013) simulated 10 heavy lake-effect snow events to examine the role of ice cover with fully frozen lakes and control simulations. In these simulations, ice cover significantly decreased downstream snowfall and served to reduce surface winds, decreasing the flux and convergence needed for lake-effect bands. The authors discovered that Lake Superior ice cover had the most widespread and strongest influence on heavy lake-effect snowfalls followed by Lake Michigan with Lake Ontario ice cover having the least influence. Wright et al. (2013) also utilized simulations of a single lake-effect snow case to examine sensitivity to the ice cover and temperature of the eastern Great Lakes. Here, it was shown that ice cover can serve to focus or enhance precipitation along the ice cover edge due to roughness changes. The lack of ice cover and increase in LSTs also generally increased the downwind extent of both the heaviest and all precipitation, along with an increase in lake-effect snow intensity. Given these studies and their findings as well as trends toward less ice cover and more open water during the winter season, there could be a longer period of time in which lake-effect snow could form. Warmer lake temperatures and less ice cover can also serve to increase the intensity of lake-effect snow, potentially increasing snowfall totals and impacts from these events.

1.4 Future Trends in Lake-Effect Snow

Some previous studies have examined future lake-effect snow changes. Kunkel et al. (2002) defined the number of grid points or events meeting criteria favorable for lake-effect snowfall near Lake Erie using numerical simulations, which revealed that the occurrences of temperatures favorable for heavy lake-effect snow are expected to decrease, while all other favorable conditions are expected to occur at about the same frequency. Notaro et al. (2015) utilized dynamically downscaled climate projections over the whole Great Lakes region under the Representative Concentration Pathway (RCP) 8.5 scenario and found a general reduction in heavy lake-effect snowstorms, with some increases around Lake Superior. However, the resolution of these projections (25 km) was too coarse to explicitly resolve lake-effect snow bands, which can be 5-50 km wide and 20-200 km long depending on the band type (Niziol et al. 1995). This means that these results could omit fine details important for lake-effect snow, such as mesoscale land/lake breezes. One study that did focus on fine-resolution (4 km) simulations of precipitation changes is Liu et al. (2017). However, their study focused on the CONUS as a whole and used the pseudo-global warming (PGW) approach (e.g., Schär et al. 1996; Rasmussen et al. 2011) to simulate a future climate under RCP8.5. As such, their simulations may not have captured important changes in weather patterns under climate change that could have large implications on lake-effect snow development.

As highlighted above, while some studies have been performed to analyze temporal trends in snowfall in a changing climate, to the best of the authors' knowledge, none have covered the entire Great Lakes region or have been conducted at a resolution fine enough to explicitly resolve lake-effect snow processes. To overcome the shortcomings of these prior studies, in this work, we focus on studying lake-effect snow specifically over the Great Lakes region with a high-resolution simulation dataset. We focus on

thermodynamic variables related to lake-effect snow, its creation, and its maintenance. We also examine changes in the properties of lake-effect snow bands such as their depth and strength, to obtain a proxy for potential changes in lake-effect lightning characteristics. Based on the prior studies of lake-effect snow and climate change impacts on temperature and precipitation, we propose three hypotheses:

H1: The intensity of lake-effect increases in some areas due to warmer, ice-free lake waters providing more instability and moisture fluxes.

H2: Lake-effect snowfall will become less common in occurrence due to warming surface temperatures, with occurrences shifting more to the core and colder winter season instead of during the transition seasons.

H3: Increased instability and warmer, ice-free lake waters will contribute to deeper lake-effect bands with stronger updrafts, perhaps increasing the chances for electrification within lake-effect storms.

The rest of this thesis will focus on utilizing various methods of analysis to test these hypotheses. Chapter 2 discusses the various methods of analysis used in this work. Chapter 3 will show results regarding possible changes in the intensity of overall snowfall and lake-effect snowfall across the Great Lakes, as well as how often conditions supportive of lake-effect snow occur and how or where they may change. Changes in the overall environments for lake-effect snow will be examined in Chapter 4, along with changes in characteristics of these lake-effect bands to conclude how impacts from these events will change in a warming climate. Finally, Chapter 5 will serve to summarize the findings of this thesis and put them in the broader context of a warming climate through their discussion.

Chapter 2

Data and Methods

This study uses dynamically downscaled general circulation model simulations conducted by Gensini et al. (2022). The simulation data cover the entire CONUS with a horizontal grid spacing of 3.75 km, 51 vertical levels, and an output interval of 15 minutes. The simulations were performed under the RCP8.5 scenario for two 15-year epochs: the historical period (1990-2005) and the end-of-century period (EOC; 2085-2100). The RCP8.5 scenario represents a high greenhouse gas emissions scenario in which radiative forcing increases by 8.5 W m^{-2} by the year 2100 and is discussed in the Intergovernmental Panel on Climate Change's (IPCC) Fifth Assessment Report (IPCC 2014). These simulations were run yearly and were continuously integrated across each hydrologic year (Oct 1st - Sep 30th). The simulations were bias corrected using 1981-2005 European Centre for Medium-Range Weather Forecasts (ECMWF) Re-Analysis (ERA) Interim data following the methods in Bruyère et al. (2014). After comparing the output of the simulations to independent observational data such as the Parameter-elevation Regressions on Independent Slopes Model (PRISM), it was found that temperature and precipitation were replicated well in the historical period. The largest temperature biases were found in daily maximum temperatures being too cold across much of the CONUS and dry biases in precipitation in the southeastern U.S. Further details and evaluation of the model can be found in Gensini et al. (2022).

The downscaled simulation data are used at 6-hour intervals in this study and subset to the domain of interest over the Great Lakes region. This domain extends

approximately between the latitudes of 40°N and 49.5°N as well as the longitudes of 93°W and 73.5°W to include all the Great Lakes as well as areas sufficiently downwind, thus capturing the main lake-effect-prone regions. When examining changes in the average snowfall or distributions, only snowfall amounts greater than 0.1 inches (2.54 mm) were used to avoid inclusion of extremely small snowfall amounts calculated by the simulation that may otherwise skew the results.

2.1 Lake-Effect Criteria Selection

To isolate the analysis to only lake-effect snow events and thus omit synoptic-scale storms, a set of favorable lake-effect snow conditions were used, similar to the methodology performed in Kunkel et al. (2002):

- The first condition is a 2-m temperature between 0 °C and -10 °C, cold enough at the surface for any precipitation to likely be falling as snow.

- The next condition is an 850-mb wind direction between 240° and 340° with a wind speed of 6 m s^{-1} or greater. This wind direction range creates favorable fetch over all of the Great Lakes necessary for lake-effect snow, with wind speeds sufficiently fast enough for enhanced heat and moisture fluxes off of the lake surfaces.

- The third condition is a 900-700-mb mean wind direction between 240° and 340° with a speed of 6 m s^{-1} or greater, similar to the previous condition. This condition serves to identify times where the mean boundary layer wind is relatively unidirectional, giving a shear criterion for our favorable lake-effect snow conditions. This is an important criterion because shear is known to disrupt or prevent lake-effect snow bands (Niziol 1987).

- The final condition is a difference in the 2-m and 850-mb temperature of 10 °C or greater, which provides a proxy for low-level instability over the lake waters that is favorable for lake-effect snow development. A 13 °C temperature differential was also examined to test for sensitivity to this threshold and to capture more intense lake-effect snow environments.

Perhaps a better proxy for instability would be the difference between the lake surface temperature and the 850-mb temperature; however, owing to data limitations, the simulated lake surface temperatures were unavailable. Hanrahan et al. (2021) showed that 2-m temperature changes largely followed lake surface temperature changes over the Great Lakes, and that perturbed colder 2-m temperatures followed from perturbed colder lake temperatures. As such, this gives confidence in utilizing 2-m temperature changes as a proxy for lake surface temperature changes and its use in our instability criteria. Owing to the fact that the lake surface temperature is typically warmer than the 2-m temperature during lake-effect snow events, our instability proxy likely serves as an underestimate of instability.

These criteria were applied to all output times and points in the model simulation dataset. When a point in the domain at a certain time met all of these criteria, that point was considered favorable for lake-effect snow. If a certain instance in time had at least one grid point in the domain that was considered favorable, then that time was considered a favorable lake-effect time. These favorable lake-effect times were then used to compare various aspects of lake-effect snowfalls between the periods of study. Different favorable grid point thresholds were tested to examine sensitivity, with the results being qualitatively constant for all tested.

2.1.1 Classifying Lake-Effect Snow Events

With lake-effect snowfall events often occurring over time periods longer than 6 hours and potentially up to days at a time it is important to quantify changes in the total event impacts, such as their duration, average snowfall, and where each event impacted. For this analysis, if a certain time had favorable lake-effect conditions present at 250 grid points or more in the domain, then that time was recorded. When multiple successive times were recorded, those times were grouped together into a classified lake-effect snow event until favorable conditions were no longer present at the 250 grid point threshold. The duration (start and end time) of each classified event and the total snowfall at each point in the domain were then recorded to perform this analysis.

2.2 Statistical Analysis Methods

To quantify statistically significant changes in the average 6-hourly snowfall during all times as well as during favorable lake-effect times, a bootstrapping approach was applied with 700 and 1000 iterations, respectively. Only 700 iterations were used for all snowfall times due to computational constraints. In this approach, the data from both the historical and EOC periods are combined, and two randomly sampled datasets are selected from the combined data with the same length of the original datasets for each period. From each group, the average snowfall difference between the two groups is calculated. All calculated differences are then shaped into a distribution and compared with the average difference from the original data. If the actual difference is outside the 99th percentile of all randomly sampled differences, then it is considered statistically significant (Efron and Tibshirani 1994).

Compositing was also performed to create soundings representing the environment at each site of interest during favorable lake-effect times for both 10 °C and 13 °C

instability criteria. This was done individually for both periods at each site by taking the times in which favorable 10 °C and 13 °C instability conditions existed. These times were then further reduced to only those in which more than 0.1 inches (2.54 mm) of 6-hourly snowfall accumulation was simulated at that site. The average atmospheric profiles up to 500 mb were then calculated during these times to create the composite soundings for favorable lake-effect snowfall times in each period. Composite soundings of a point 50 km upwind of each site and over the lake waters were also created to represent the over-lake environmental changes. Here, the 850 mb wind direction from each site's composite sounding was utilized as the "upwind" vector and a point in this direction 50 km from each site was found. At each upwind point, the average atmospheric profile up to 500 mb was then calculated during the same times utilized to create the over-site composite soundings.

Chapter 3

Lake-Effect Snowfall

This chapter focuses on the changes in snowfall and lake-effect snowfall in the Great Lakes region. Overall snowfall and its changes across the domain of study are examined before examining changes in lake-effect snowfall. The sensitivity of the results to different instability criteria are examined along with the classification of lake-effect snow occurrences into continuous events. Finally, individual sites of interest across the Great Lakes are investigated to understand changes in snowfall impacts from all snowfalls and favorable lake-effect snowfalls with both instability criteria. The content within sections 3.1, 3.2, and 3.3 are replicated from Laurinaitis et al. (2025; in prep.).

3.1 Overall Changes in Snowfall

Figure 3.1 shows the domain of interest in this study, which spans the 5 Laurentian Great Lakes. In addition to domain-wide analyses, we select 2 sites for each lake in areas prone to lake-effect snow for site-specific analyses, and these 10 sites are also shown. The snowfall amounts corresponding to specific percentiles of 6-hourly snowfall are shown for each site and for each study period.

For locations off Lake Superior and Lake Huron (shown by the top row of sites in Figure 3.1), an increase in the snowfall amount corresponding to the higher percentiles is seen in the EOC period compared to the historical period. The increase is shown to be the greatest for the Owen Sound and Midland sites located off Lake Huron, with

the 95th and 99th percentile snowfalls at Owen Sound increasing by nearly 15 mm/6hr and 40 mm/6hr, respectively. The sites along the other lakes show much less or no difference in the snowfall amounts at the highest percentiles between the two periods. This indicates that locally along the northern lakes (Superior and Huron), higher-end snowfall events are expected to become more intense in the future under a warming climate.

To test H2, Figure 3.2 shows the spatial distribution of relative changes in the seasonal average snowfall amounts for the fall (September, October, and November; SON), winter (December, January, and February; DJF), and spring (March, April, and May; MAM) seasons. In SON, widespread relative decreases in season-total snowfall can be seen, with magnitudes of 50% or greater in some areas by EOC. Areas downwind of the lakes in Michigan show less of a decrease, which could be an indicator of enhanced lake-effect snow offsetting the general decrease in snowfall by EOC. In DJF, a relative decrease in season total snowfall is still seen across much of the domain, albeit at a lesser extent compared to SON. Coastal areas downwind of Lake Superior and Lake Huron show an increase in season-total snowfall by EOC in prominent lake-effect snow regions. Similar to SON, season-total snowfall amounts in MAM show a relative decrease across most of the domain by EOC. The magnitude of this change is less than that of SON but is still greater than those found during DJF. Some regions of little to no change in seasonal snowfall are apparent yet seem to be synoptically forced in nature due to their spatial extent and locations.

It is apparent from the changes displayed in Figure 3.2 that snowfall in general across the Great Lakes region is expected to undergo a temporal shift in the future, with lower amounts in the transition seasons of SON and MAM and potentially increased lake-effect snow in DJF. This is consistent with the effects of climate warming, as the

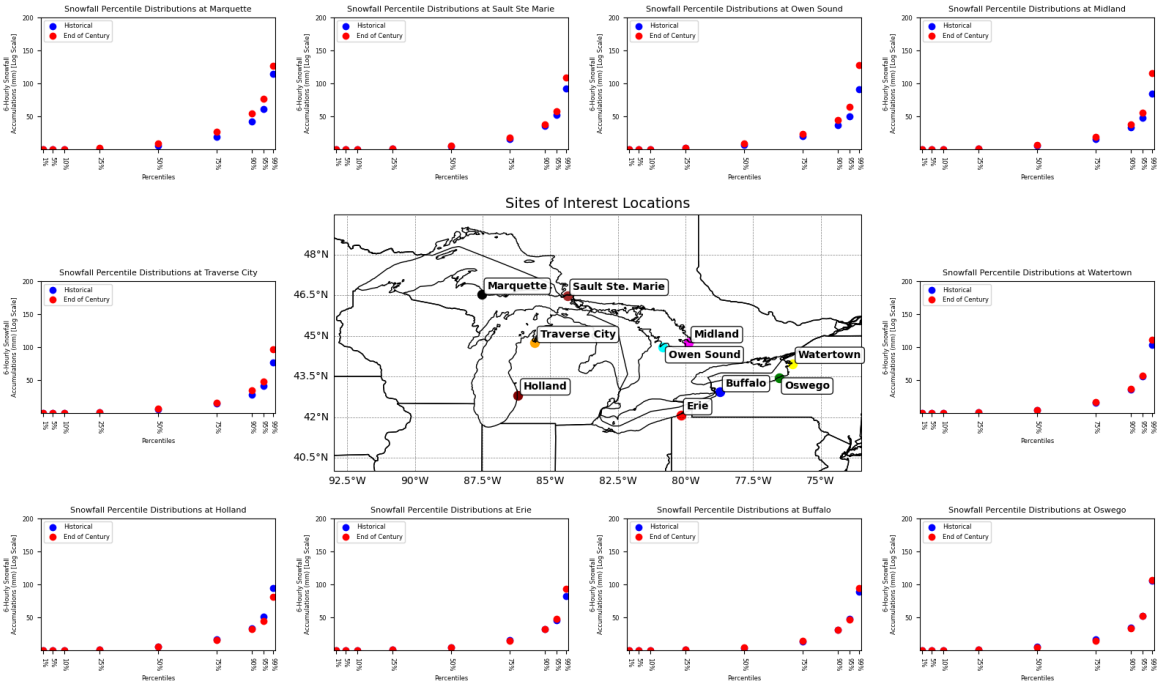

Figure 3.1: Central plot depicts the study domain, including locations of the sites prone to lake effect snow used in this study. Surrounding plots compare the snowfall amounts corresponding to various percentiles of 6-hourly snowfall accumulations at each site in the historical (blue) and EOC (red) periods.

period of time each year in which it is cold enough for snow is expected to decrease—temperatures cold enough for wintry weather would be more confined to the coldest months of the year. Snowfall changes can also be seen spatially with the lake-effect snow belts off Lakes Superior, Huron, and Michigan showing a less of a snowfall decrease in SON and MAM and even an increase in snowfall increase during DJF. Based on these results, it can be inferred that snowfall from synoptic systems in the Great Lakes will decrease in a warming climate while lake-effect snowfall will increase off some of the lakes.

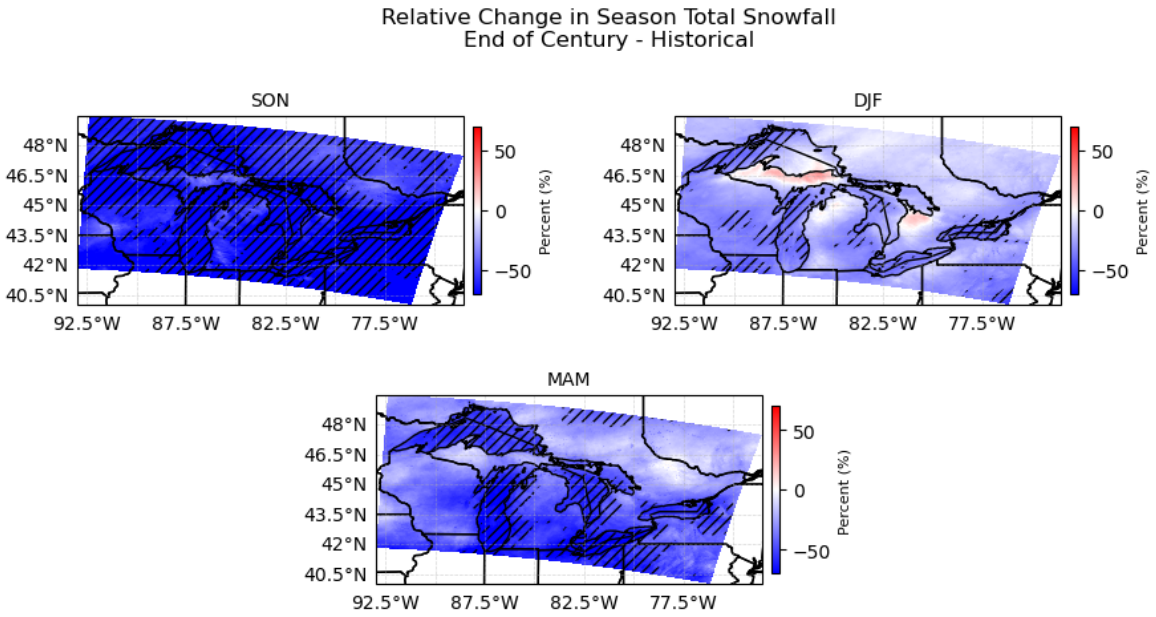

Figure 3.2: Spatial distribution of relative changes in the seasonal average snowfall accumulation between the EOC and historical periods for (a) SON, (b) DJF, and (c) MAM (units: %). Hatching signifies significant changes at the 99% confidence level with 10000 iterations using the bootstrapping approach summarized in the Data and Methods Chapter 2.

3.2 Changes in Lake-Effect Snowfall

The above analysis shows relatively large decreases but also some increases in seasonal snowfall amounts, and the sign of the change is shown to be dependent on the time of year (season) and geographic location (lake). However, what remains unclear is what causes these changes in the lake-effect snow belts that may be influenced by changes in lake-effect snow. Therefore, the changes in the conditions favorable for lake-effect snow with 10 °C instability are shown in Figure 3.3, with further analysis exploring sensitivity to a change in instability to 13 °C found in section 3.4. In the EOC period, there is a domain-wide decrease in occurrences of 2-m temperature below freezing compared with the historical period (Figure 3.3a), as expected with climate warming. This decrease is even more pronounced over the lakes themselves, with the largest decreases found over much of Lakes Superior and Michigan. This decrease in occurrence of temperatures below freezing contradicts the regional increases in snowfall shown in Figure 3.2. The larger decreases in snowfall over the lakes shown in Figure 3.2 are likely related to decreases in ice cover and thus warmer lake surface temperatures. These areas also coincide with increases in the number of instability events favorable for lake-effect snow (temperature differential between 2-m and 850 mb exceeding 10 °C), with increasing occurrences found over Lake Michigan and Lake Huron, and especially Lake Superior, as shown in Figure 3.3b. As lake surface temperatures and 2-m temperatures warm with ice-free lakes, and little to no change in the 850-mb temperatures, ample instability will be present more often for lake-effect convection to initiate. Elsewhere across Lake Erie and Lake Ontario, the changes are small or show roughly the same occurrence between the historical and EOC periods.

When examining favorable boundary layer wind directions for lake-effect snow, a domain-wide decrease in the occurrence of favorable conditions is found (Figure 3.3c,d).

However, this decrease is not noticeably large in regions over and downwind of any of the Great Lakes and as a result likely has little impact on the change in total events with favorable lake-effect conditions. Combining all the conditions together (Figure 3.3e), a spatial pattern most similar to that of the instability changes is seen. By EOC, events meeting all conditions are expected to increase greatly over nearly all of Lake Superior. Over the other lakes the number of occurrences generally decreases, with widespread decreases over most of Lake Ontario and Lake Erie. Given the general consistency between changes in the occurrence of unstable conditions and the number of instances where all lake-effect snow conditions are met, this suggests that the change in the frequency of favorable instability for lake-effect snow is the main driver of the change in lake-effect events across the Great Lakes in a warming climate.

In addition to the increase in the occurrence of instability over the northern lakes by EOC, 10-m winds are also found to converge more on the downwind shores of each lake during favorable lake-effect times in the EOC period (Figure 3.3f). These areas of increased convergence also extend over the water in the eastern portions of Lake Superior and Lake Huron. Increased convergence near the surface could serve to form stronger updrafts and more confined precipitation regions in lake-effect storms, leading to heavier snowfall rates within these bands. The monthly frequency of all conditions being met is also shown to decrease overall by EOC in Figure 3.3g. However, the number of events in the DJF season increases by EOC, while the number decreases in the transition seasons (SON and MAM). As shown previously in Figure 3.3e there is also a spatial dependence on where the frequency of all conditions is increasing, with there also likely being a seasonal dependence locally in these areas. This again shows the temporal shift in snowfall across the Great Lakes, with favorable lake-effect conditions now being more confined to the climatologically coldest months of the year and increasing in number, i.e., lake-effect snowfall transitions from a bimodal temporal

distribution with peaks in late fall and late winter to a unimodal distribution with a peak in the middle of winter.

Figure 3.1 shows changes in the amount of snow associated with certain percentiles for specific lake-effect-prone sites. A question that remains is how robust are these changes spatially. To address this, spatial distributions of changes in the high-percentile snowfall levels are shown in Figure 3.4, which can be used to determine where 6-hourly snowfall is becoming more or less intense by EOC during favorable lake-effect times. All percentiles examined here show similar spatial patterns of change across the Great Lakes, with increases in the northern part of the domain and over the lakes as well as decreases over the land portions of the domain. Greater increases in the snowfall amount corresponding to the high percentiles can be seen across the Upper Peninsula of Michigan as well as off of Lake Huron into parts of southern Ontario. These increases occur in the downwind regions of the lakes and in well-known snow belts. The increases are also relatively confined in nature and show the spatial footprint of heavier lake-effect bands across the regions. For the top 1% of favorable lake-effect snowfall accumulations, 6-hourly accumulations increase by 50 mm or more off Lake Superior, with similar magnitudes off Lake Huron. This is similar to the percentile changes shown previously at the Superior and Huron sites for all 6-hourly snowfall amounts. As such, these results again indicate an increase in intensity in the higher-end snowfall events in the future under a warming climate, and the results are generally broadly applicable over large areas of each lake, not just individual sites. This is especially the case off the lakes mentioned previously with lesser changes in intensity found over others, such as Lakes Erie and Ontario. This result and those found in Figure 3.2 indicate that lake-effect snow across the northern lakes is expected to increase in magnitude and intensity in a warming climate, with seasonal snowfall increases occurring due to these increases.

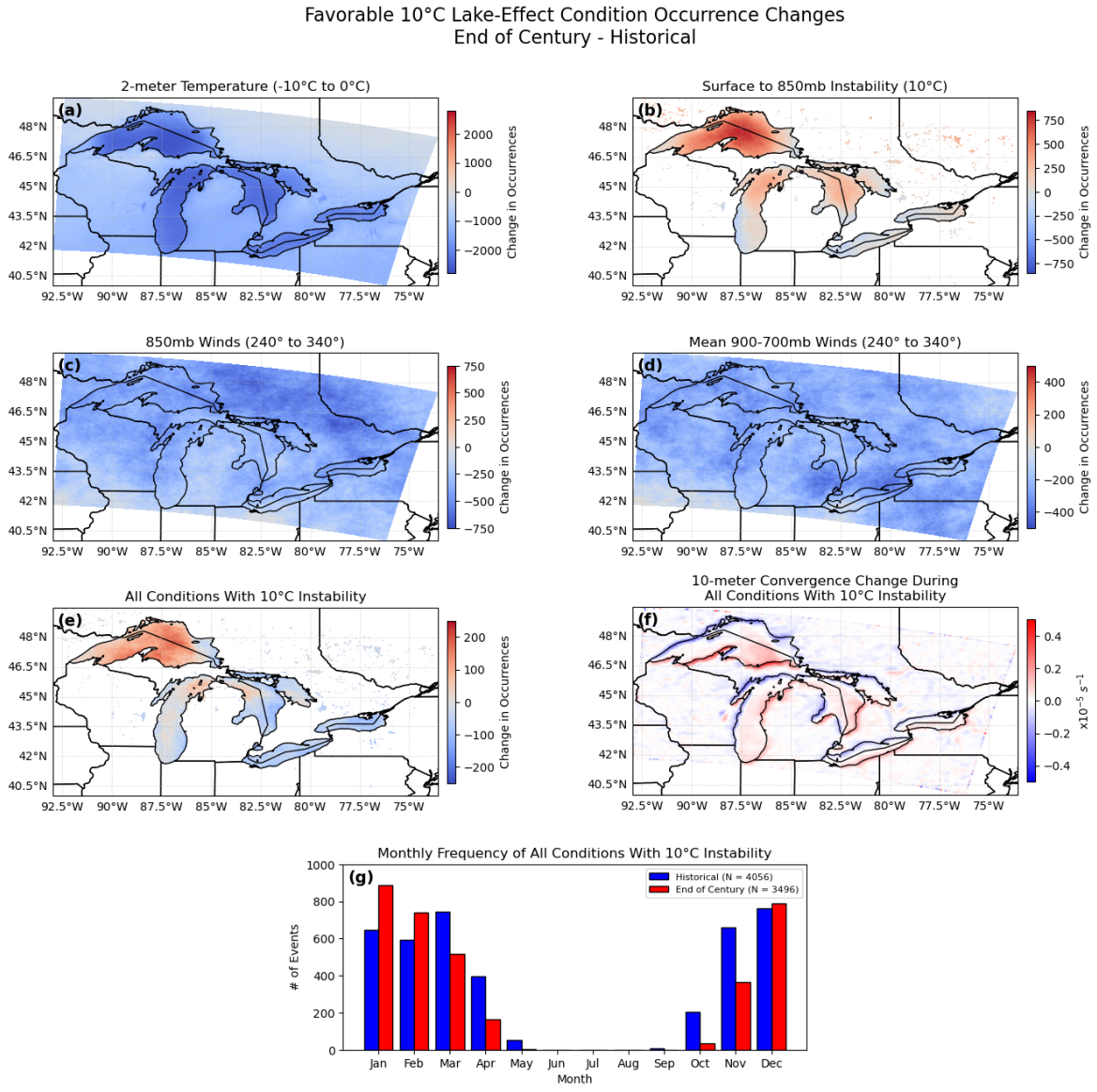

Figure 3.3: Spatial distribution of the changes (EOC minus historical) in the number of occurrences of the a) favorable temperature criterion, b) favorable instability criterion, c) favorable 850 mb wind criterion, d) mean favorable 900-700 mb wind criterion, and e) all favorable criteria being met as well as the change in average 10-m convergence during favorable lake-effect times in panel f. Panel g shows a monthly occurrence histogram of times when all conditions are met with the 10 °C instability criteria for the EOC and historical periods in red and blue, respectively.

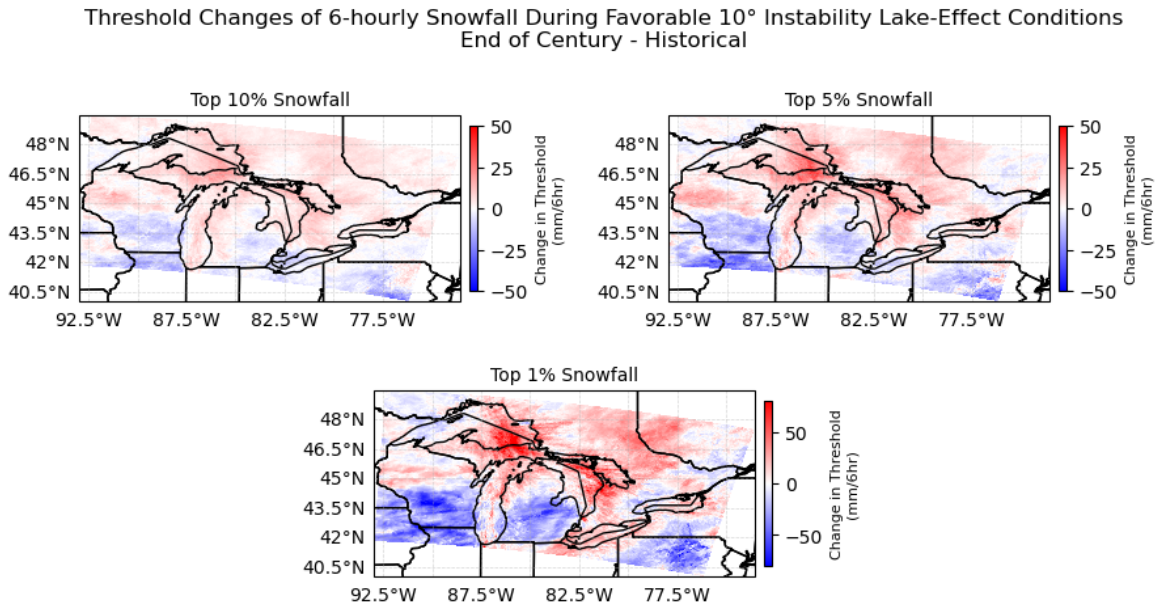

Figure 3.4: Spatial distribution of changes in the top 10, 5, and 1% 6-hourly snowfall accumulations during favorable lake-effect conditions with the 10 °C instability criteria (EOC - Historical). The change in the snowfall accumulation corresponding to each percentile is shown in mm per 6 hours.

Figure 3.5 compares the spatial distributions of changes in the average 6-hourly snowfall accumulations for all snowfall events and only favorable lake-effect events with 10 °C instability. When all occurrences of snowfall are included, a domain-wide decrease in the average snowfall is seen, with large decreases over much of Lake Superior by EOC. This large decrease is likely the result of warmer lake water temperatures and less ice cover, as mentioned above. Despite this, there are some locations along the Upper Peninsula of Michigan and off Lake Huron south of the Georgian Bay where the average snowfall stays roughly the same or even increases by EOC. Off Lake Superior, this increase in average snowfall intensity is more clearly seen. This shows that even when all snowfall events (synoptic, lake-effect, lake-enhanced, etc.) are included in the analysis, a signal of increased snowfall in some areas prone to lake-effect snow remains.

Looking at only the favorable lake-effect snow times, a similar spatial pattern of statistically significant average snowfall increases is present. Significant increases are seen over more of the Upper Peninsula, south of the Georgian Bay, and over eastern Lake Superior itself. Some increases in average 6-hourly snowfall are also seen in the snow belts off Lake Michigan, albeit at a lesser magnitude. Elsewhere across the domain, the changes in average snowfall are small and are not significant, with no large decreases in snowfall found anywhere. From this analysis it can be seen that lake-effect snowfalls are expected to maintain their intensity in a warming climate across most of the Great Lakes, with several regions experiencing an increase in snowfall intensity. Factors leading to this include increases in instability in these regions as well as low-level convergence near the shorelines of these lake-effect prone regions, as previously shown in Figure 3.3.

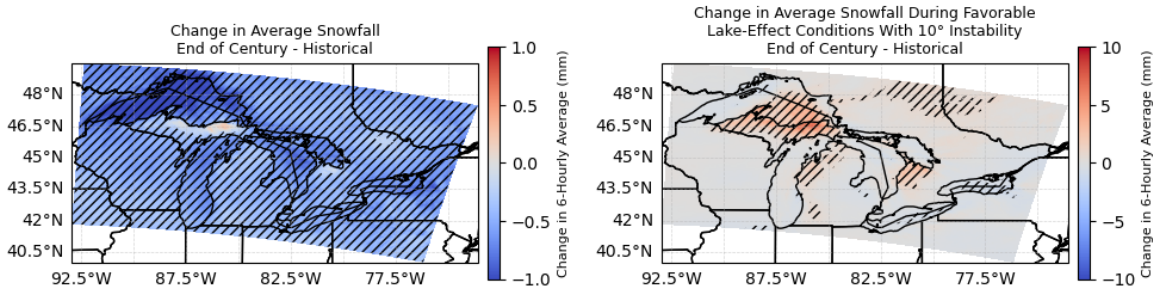

Figure 3.5: Changes in the average 6-hourly snowfall accumulation during all snowfall periods (left) and during favorable lake-effect conditions with the 10 °C instability criterion snowfalls (right) between periods (EOC - Historical). Hatching signifies significant changes at the 99% confidence level using the bootstrapping approach summarized in the Data and Methods Chapter 2.

3.3 Changes in Classified Lake-Effect Snow Events

The parameters of lake effect snow have been examined and how they can change in a warming climate, and increases in its intensity have been seen in some regions of the Great Lakes. However, many lake-effect snow events can occur over timescales much longer than 6 hours and up to days at a time. As such, it is also important to examine how entire lake-effect events can change in a warming climate using the methods discussed in the Section 2.2. The results of this analysis are shown in Figure 3.6, where the changes in various parameters of classified favorable 10 °C instability lake-effect snow events are shown. The change in the occurrences of lake-effect snow events can be seen in Figure 3.6a, with decreases in the number of events domain-wide. A larger magnitude of decreases is present over portions of the eastern lakes, such as Lake Ontario and Lake Erie. However, Figure 3.6b shows that even though the number of lake-effect snow events is expected to decrease, the average event total snowfall over certain areas, especially lake-effect-prone areas off of Lake Superior, Lake Huron, and Lake Michigan, increases by EOC, with little to no change across the rest of the domain. In parts of the Upper Peninsula of Michigan, the average event total

snowfall is found to increase by 50-70 mm by EOC. This is consistent with the locations showing increased average 6-hourly lake-effect snowfall intensity shown in Figure 3.5.

The number of classified events per season is also presented for each period. Here, a general decrease in the number of classified lake-effect snow events per season is present, with an average of 32.5 events per season in the historical period and 25.9 events per season by EOC. However, the spread in the average event total snowfall distributions increases in the EOC period based on the inter-quartile ranges of the distributions for most seasons. The distribution of average event total snowfalls over the entirety of each period is shown in Figure 3.6e. Here, a similar result is seen with higher average event total snowfalls in the EOC period with the tail of the distribution much further spread than in the historical period, and the average event snowfall totals are upwards of 150 mm. Furthermore, the distribution of the classified lake-effect snow event durations is presented in Figure 3.6f, and again a decrease in the total number of classified lake-effect snow events is found by EOC. Within the EOC period, a slight skew in the distribution toward longer-duration events can be seen compared to the historical distribution. However, the distributions are not significantly different at the 90 or 95% confidence level.

The results from this analysis indicate that within a warming climate, fewer lake-effect snow events may occur overall across the Great Lakes. However, these events will tend to either remain the same in intensity or will increase in intensity in regions off of Lake Superior, Lake Michigan, and Lake Huron. Lake-effect snowfall events may also become more variable spatially and may slightly increase in duration, all of which changes the localized impacts of these snow events in a warming climate.

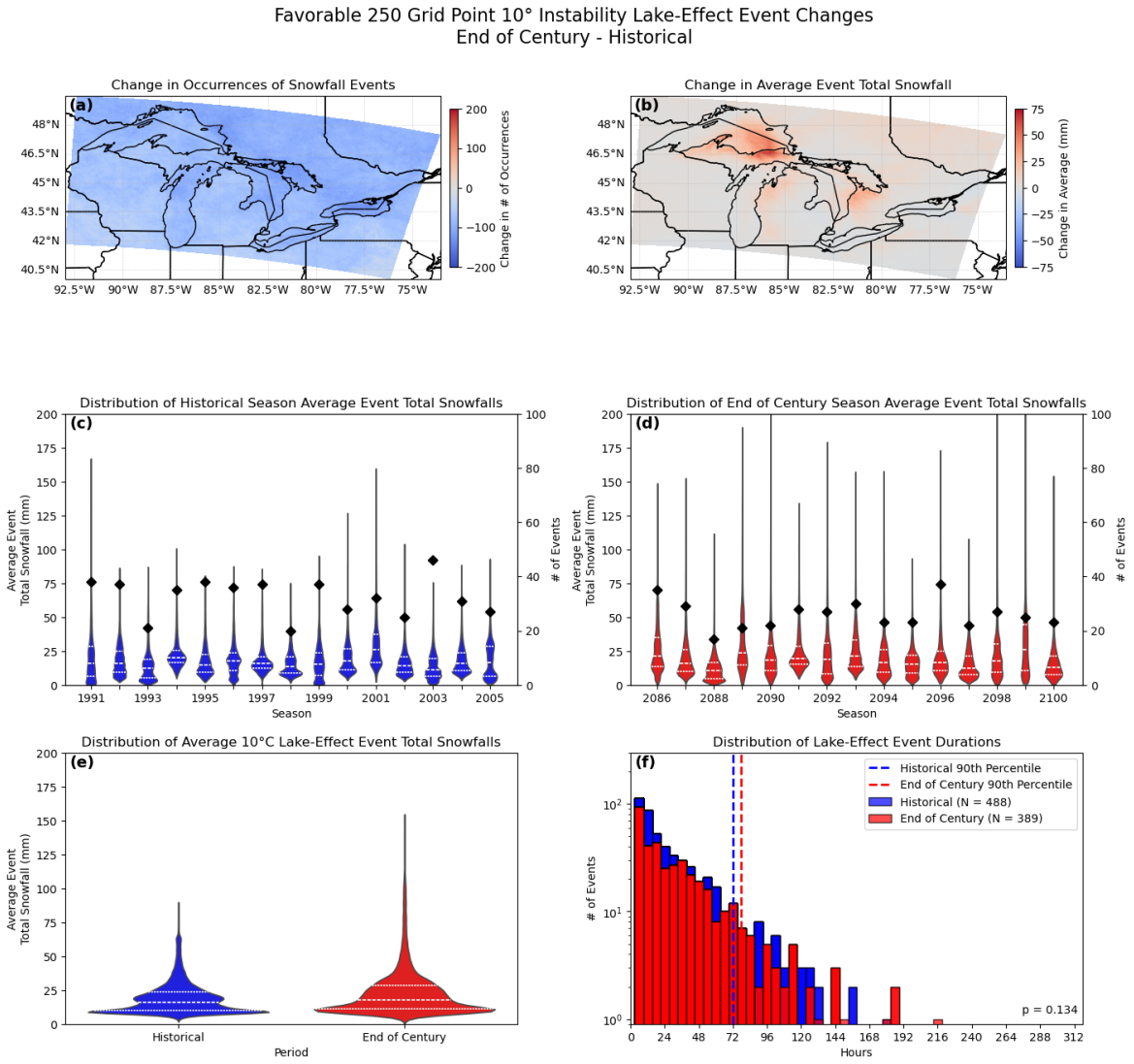

Figure 3.6: Changes in (a) the occurrences of and (b) the average event total snowfall for classified favorable 10 °C instability lake-effect events. The distribution of the average event total snowfalls over the domain in each winter season as well as the number of classified events per season (diamonds) is shown for both (c) the historical and (d) EOC periods as violin plots. A season year is defined as the year of the JFM months in a given winter season, where a winter season contains events from October to May. The distribution of average event total snowfalls over each entire period is shown in panel (e) as violin plot. White dashed lines in the distributions show the quartiles of each distribution. The distribution of the durations of the classified lake-effect events for each period is shown in panel (f), with the resulting p-value from a 2-sample Kolmogorov-Smirnov test for significant changes in the distributions in the bottom right of the panel.

3.4 Sensitivity to Instability Thresholds

Thus far, this work has focused on changes in lake-effect snow with an instability criterion of 10 °C to capture a wide range and sample of possible lake-effect events with our modified definition of instability using 2-m temperatures instead of lake surface temperatures. Here, we begin to examine the changes in lake-effect snow properties but instead with the widely used instability threshold of 13 °C for lake-effect processes to initiate (Niziol 1987), allowing us to test the sensitivity of the results to the instability parameter. Using this higher instability threshold will also allow examination of the possible changes in more extreme and higher-end lake-effect events only.

Figure 3.7b shows the change in occurrences across the lakes of the surface to 850 mb instability being greater than 13 °C. Here, a different pattern is apparent than that found in the 10 °C instability changes (Figure 3.3b), with increases across most of Lake Superior, Lake Huron, Lake Erie, and the eastern part of Lake Michigan. Over Lake Ontario, widespread decreases in the number of occurrences are found with the largest found in the southeastern portion of the lake. When looking at the change in all conditions being met together with 13 °C instability (Fig. 3.7e) a very similar spatial pattern to that found in the instability changes is seen. Again, slight increases in the number of occurrences of favorable lake-effect conditions are seen across Lake Huron, Lake Erie, and parts of Lake Superior and Lake Michigan. All of Lake Ontario is expected to have fewer occurrences of all conditions together, again showing the consistency between unstable conditions and all lake-effect conditions being met. As shown previously with the 10 °C favorable condition changes (Figure 3.3), this suggests that the change in the frequency of favorable instability and favorable surface temperatures is mainly driving changes in lake-effect snow events in a warming climate.

Likewise, 10-m winds are found to again converge more on the downwind shores of each lake during 13 °C lake-effect events by EOC (Fig. 3.7f). The convergence change is spatially similar to the change found during 10 °C lake-effect events, with the magnitude of changes now larger and more convergence is found over the actual lake waters. This increasing convergence over the lake waters may assist in the development and intensification of lake-effect bands further out over the lakes before they reach the shore. When reaching the shore, larger amounts of convergence can serve to deepen and intensify lake-effect bands even more, producing precipitation regions containing heavy snowfall rates. Figure 3.7g shows the monthly frequency of all the 13 °C conditions being met and, as expected, we see fewer occurrences in each period meeting these conditions compared to the 10 °C conditions, with about a 90% decrease in each period. However, similar changes in temporal variability are seen with increases in the occurrences of favorable conditions during the core winter months and sharp decreases in other months. Here, the shift in favorable lake-effect conditions to the core winter season by EOC is again seen, with lake-effect snow expected to become less common in the transition seasons.

The spatial distribution of the changes in certain high-percentile 6-hourly 13 °C lake-effect snowfalls is shown in Figure 3.8. Similar to the changes in percentile snowfalls for 10 °C lake-effect times (Figure 3.4), each of the percentiles is spatially similar, with the largest increases in higher-end snowfall intensities found downwind of Lake Superior and Lake Huron. Some increases are seen downwind of Lake Erie and especially Lake Ontario in the top 1% of favorable 13 °C lake-effect snowfalls, with increases seen over part of central New York and the Tug Hill Plateau. As opposed to the 10 °C snowfall changes, any increases in the intensities are strictly located over or downwind of the lakes. This gives support that the times being examined here are nearly all lake-effect

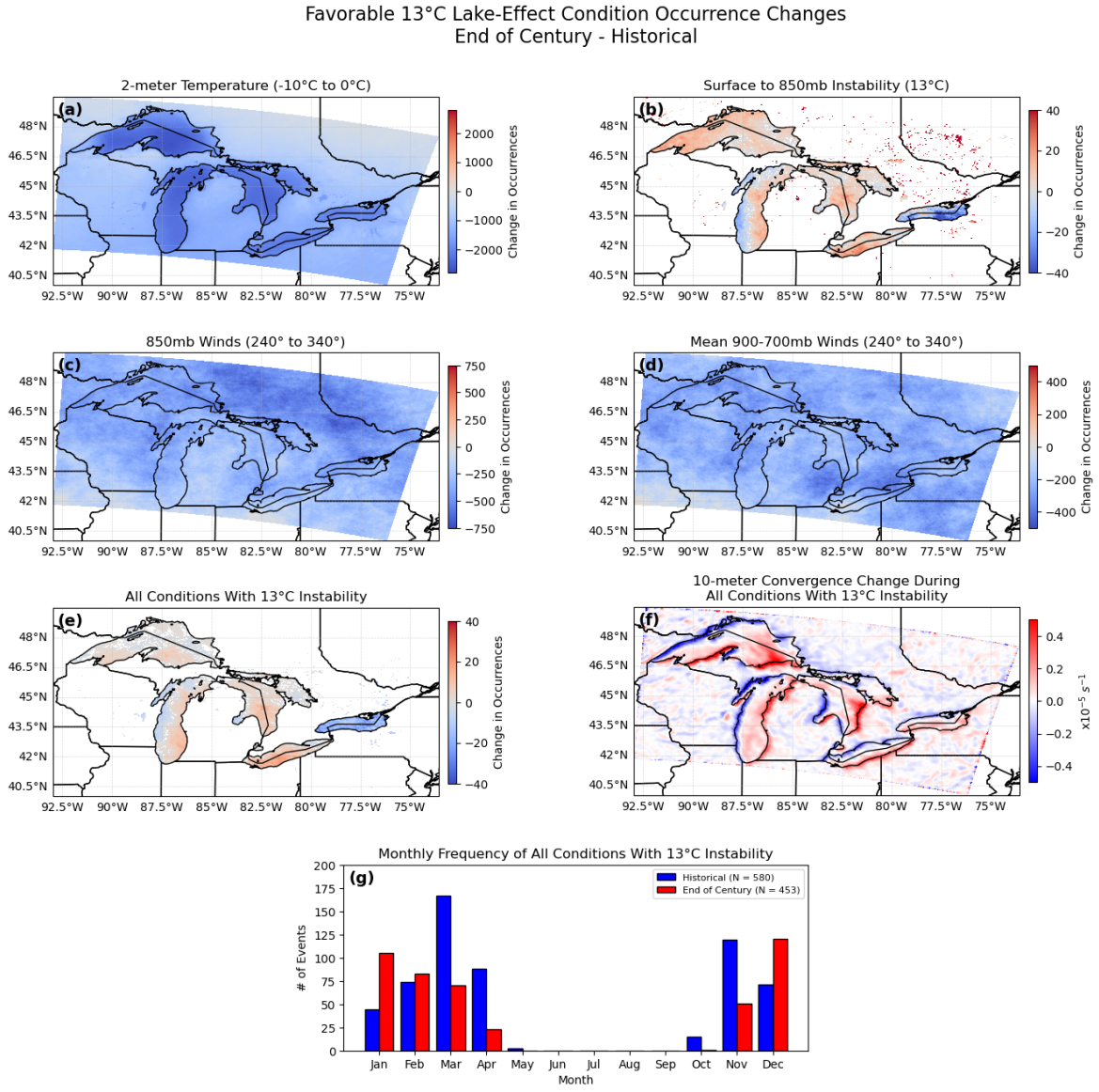

Figure 3.7: Same as Figure 3.3 but for the favorable 13 °C lake-effect snow criteria. Panels a, c, and d are the same as in Figure 3.3.

in nature and that it is explicitly lake-effect intensities that are increasing in a warming climate, as also seen by the narrow "banded" spatial changes. The highest increases in the intensity of the top 1% lake-effect snowfalls are upwards of 100 mm/6hr or more near the Upper Peninsula of Michigan and parts of southern Ontario, corresponding to an increase of nearly 4 inches per 6 hours and 0.67 inches per hour when averaged. This again supports the idea that lake-effect snow is expected to increase in intensity across portions of the northern Great Lakes in a warming climate and that this change in intensity is what is driving seasonal snowfall increases in prominent lake-effect snow belts.

A comparison of the changes in the average 6-hourly snowfall accumulations during all times in the data and during only favorable 13 °C lake-effect times is shown in Figure 3.9. As mentioned previously a significant near domain-wide decrease is seen in the average overall snowfall by the EOC, with some minor increases or negligible changes across the Upper Peninsula of Michigan and in a small area downwind of Lake Huron. When examining the change in the average 13 °C lake-effect snowfall, we see significant increases off Lake Superior, Lake Huron, and Lake Michigan with magnitudes greater than those found in the average 10 °C instability lake-effect snowfall (Figure 3.5). Increases in the average 13 °C lake-effect snowfall are also now present downwind of Lake Erie and Lake Ontario, with some of them significant. These changes were not present in the average 10 °C lake-effect snowfalls shown in Figure 3.5 and indicate that the snowfall that occurs in more intense lake-effect environments is expected to increase in these regions, while in the more common lake-effect environments, it is expected to remain roughly the same. This result matches well with those seen in Figures 3.4 and 3.8 where the increases in the average 6-hourly snowfall at certain thresholds are mostly only seen at the highest thresholds off these two lakes.

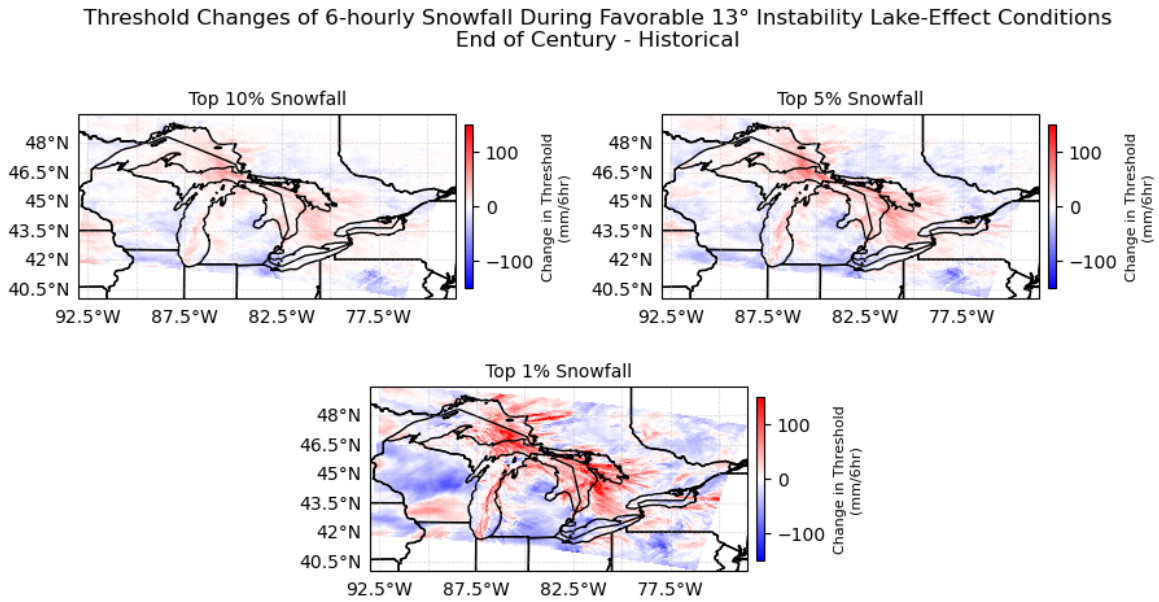

Figure 3.8: Same as Figure 3.4 but for favorable 13 °C lake-effect snow criteria.

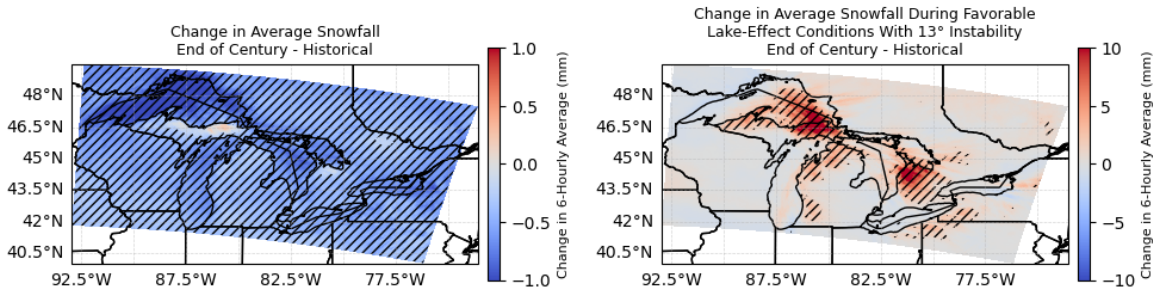

Figure 3.9: Same as Figure 3.5 but for snowfalls during favorable lake-effect conditions with the 13 °C instability criteria.

These 13 °C lake-effect snowfall occurrences are then classified into continuous events in the same fashion as those examined in Figure 3.6 for 10 °C events, and Figure 3.10 shows the changes in various measures of snowfall in these events. Figure 3.10a in this figure shows the changes in the number of occurrences of these events, and decreases in the number of events can be seen across much of the domain. Some minor increases are present across the southern portion of the domain with some possibly due to the inland extent of lake-effect snowfall increasing in a warming world with more intense lake-effect snow events (Wright et al. 2013). As inland extent may increase by EOC, more occurrences of snowfalls further away from some of the lakes may be due to lake-effect events than in the historical period. As a result, the occurrences of snowfall events increase in certain regions, such as the southern greater Toronto metro area and south-central Michigan. When examining the change in the average event total snowfall during 13 °C lake-effect events in Figure 3.10b, a very similar spatial pattern to that shown in the 10 °C lake-effect events in Figure 3.6 is seen. These increases in average event total snowfall are now larger downwind of Lake Superior, Lake Huron, and Lake Michigan with some increasing by nearly 75 mm (around 3 inches) by EOC. Off Lake Erie and Lake Ontario, some minor increases are now also present that were not present or were difficult to see previously. The increases in average event total snowfall off Lake Huron also extend slightly further inland than those in the 10 °C lake-effect events, perhaps as a result of the increasing inland extent of lake-effect snowfall mentioned earlier.

Figures 3.10c and 3.10d show violin plots of the domain-wide distribution of average event total snowfalls per season for the 13 °C lake-effect events. Some seasons, such as 1992 and 1993 in the historical period and 2088, 2093, and 2094 in the EOC period, are not shown in these plots as there were no events in those seasons that met our classified criteria. This may be a result of utilizing 2-m temperatures instead of lake surface

temperatures for the instability criterion in this work, as these seasons may have had events that were not as unstable as in others. When using lake surface temperatures the actual instability in these cases may be over 13 °C but this is not captured due to our more stringent criterion utilizing 2-m temperatures. Of those seasons remaining, we again see an overall decrease in the number of events per season with an average of 5.3 events in the historical period and 4.0 events in the EOC period. Similar to those in the 10 °C lake-effect events, the spread in the 13 °C average event total snowfall distributions increases by EOC, although the distributions themselves are influenced more by extreme values on the tails of the distribution due to smaller sample sizes in each season. It can also be seen that the highest averages in the distributions are increasing by EOC, with some average event totals exceeding 200 mm (7.87 in) while in the historical period, no average event totals reached near this value.

When looking at the distributions of the average 13 °C lake-effect event total snowfalls over each individual period (Fig. 3.10e), we again see an increase in the spread of average event totals with higher outlier values upwards of 125 mm (4.9 in) and an increase in the inter-quartile range. Finally, the distribution of the durations of the classified 13 °C lake-effect events is shown in Figure 3.10f. Compared to the total number of 10 °C classified events, there are about 85% less 13 °C classified events. As a result the distribution is smaller and less smooth. The durations of these events are also much shorter than those of the 10 °C events, with the longest 13 °C classified events only lasting 48 hours. Looking at the duration distributions a more skewed change is seen between the historical and EOC periods, with the 90th percentile duration increasing by 12 hours between the two. This result may be due to smaller sample sizes making the distribution more skewed by higher values and the two distributions are

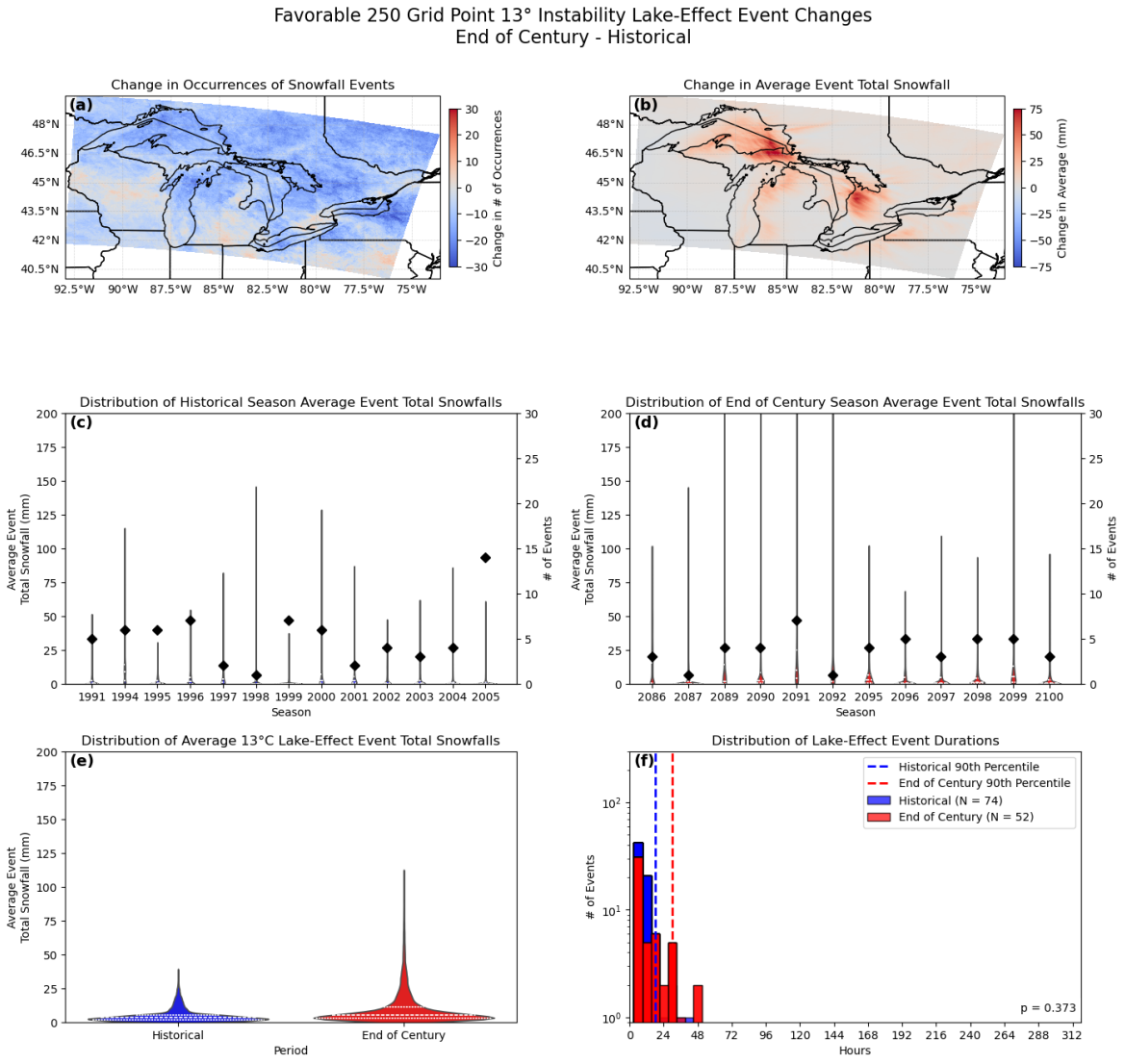

Figure 3.10: Same as Figure 3.6 but for classified favorable 13 °C instability lake-effect events.

not significantly different, however it matches the change in durations found previously in Figure 3.6 with 10 °C classified lake-effect snow events.

3.5 Site Snowfall Comparisons

Additionally the snowfall received at each of our sites of interest by the different criteria that have been utilized in this study thus far can be examined. This allows comparisons between sites regarding how much snowfall they receive in a season, how much of that snowfall comes from possible lake-effect from both instability criteria, and how these snowfall totals may change in a warming climate. The season total snowfall time series during the historical period for each site of interest is shown by Figure 3.11, with contributions from each instability criteria also shown. A split is seen between sites off Lake Michigan (Traverse City, Holland), Lake Erie (Buffalo, Erie), and Lake Ontario (Watertown, Oswego) and those off Lake Huron (Owen Sound, Midland) and Lake Superior (Sault Ste. Marie, Marquette) with the former having higher season total snowfalls and slightly higher season total snowfalls from favorable lake-effect times compared to the latter. Also of note is the greater inter-annual variability in favorable lake-effect snow totals at these sites, with more constant lake-effect snow contributions at sites off Lake Michigan, Lake Erie, and Lake Ontario. At each of the sites, less than 1000 mm of snow falls in any season during favorable 13 °C lake-effect times in the historical period.

When comparing the historical seasonal snowfall times series at each site in Figure 3.11 with the EOC seasonal snowfall time series shown in Figure 3.12, some key changes are noticed. The seasonal snowfall totals at sites off Lake Ontario (Watertown, Oswego) and Lake Erie (Buffalo, Erie) decrease the most, with lesser decreases at the sites off Lake Michigan (Traverse City, Holland) and at Sault Ste. Marie by EOC. Off Lake

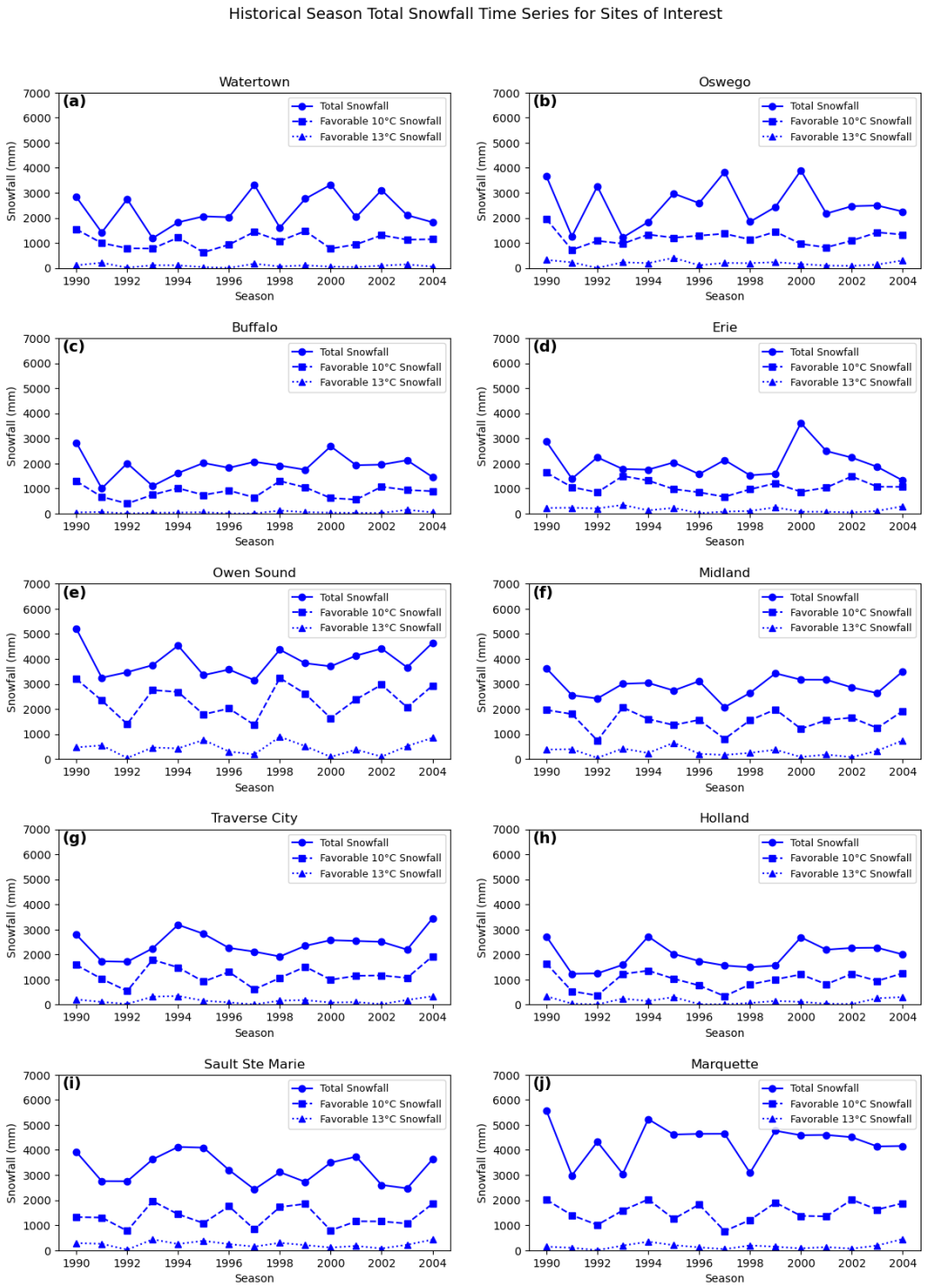

Figure 3.11: Season total snowfall time series during the historical period for each site of interest from all snowfall (solid line, circle marks), snowfall during favorable 10 °C instability criteria times (dashed line, square marks), and snowfall during favorable 13 °C instability criteria times (dotted line, triangle marks).

Huron (Owen Sound, Midland), the seasonal snowfall totals at each site remain about the same, with seasonal totals at Marquette perhaps slightly increasing with more inter-annual variability. The seasonal total contribution of snowfall during favorable lake-effect times also remains roughly the same at each site or even increases at some sites, such as those off Lake Huron and at Marquette. The percentage of total seasonal snowfall contributed by favorable lake-effect times also increases across all sites, with nearly all seasons having 50% or more of the total snowfall occurring from favorable 10 °C snowfall at every site. This indicates that in a warming climate, lake-effect processes may become the main or prominent source of snowfall at sites like these across the Great Lakes. These results also match up well with those shown previously with seasonal snowfall total changes and average 6-hourly snowfall intensity changes—lake-effect snow seems to become less common but at the same or greater intensity and contributes more to overall snowfall in some regions downwind of the Great Lakes. It has also been shown that our results for the favorable 13 °C instability lake-effect times are qualitatively similar to those for the favorable 10 °C instability lake-effect times, increasing our confidence in this changing signal of snowfall in the Great Lakes and that it is coming primarily from changes in lake-effect snow.

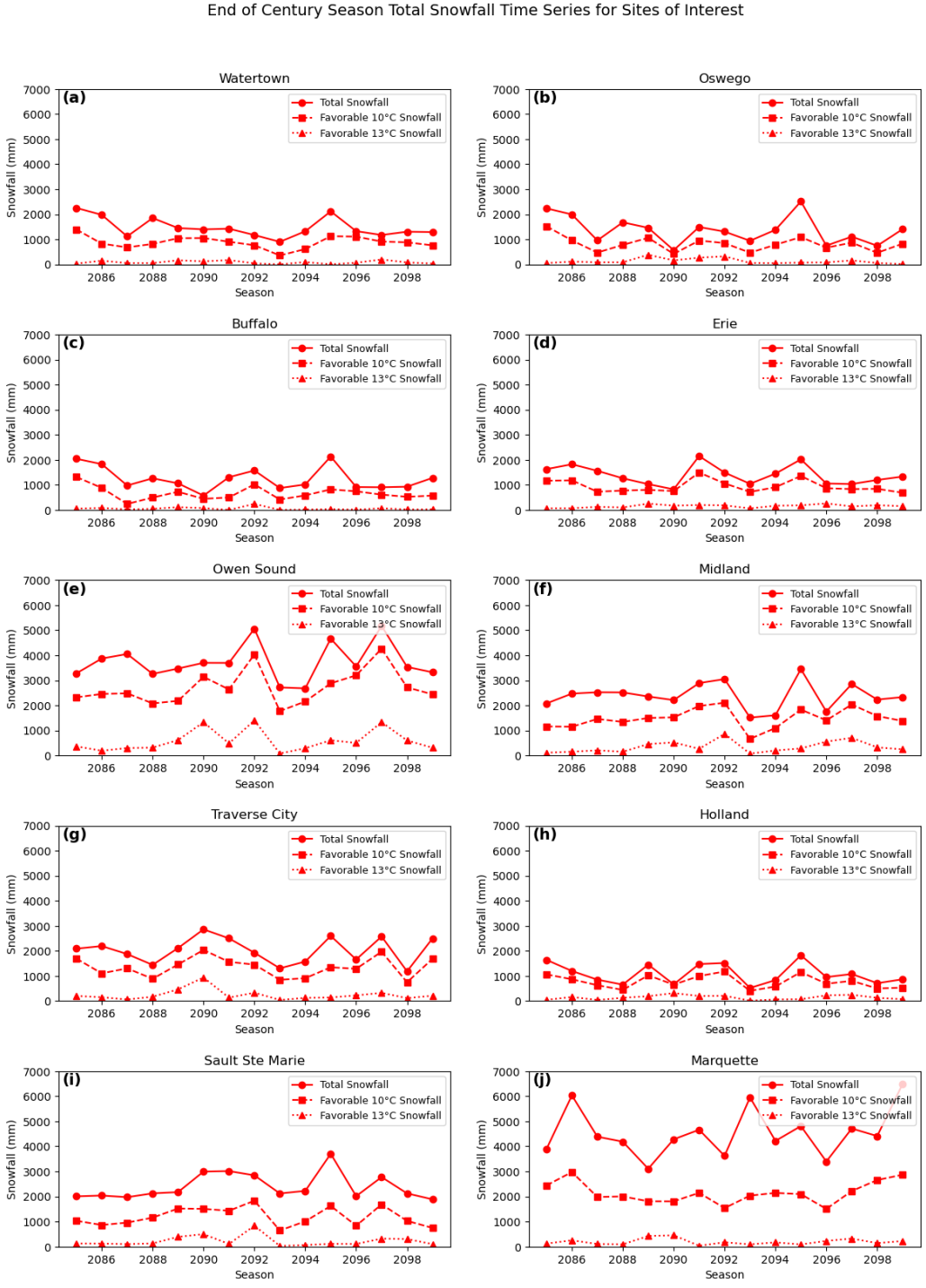

Figure 3.12: Season total snowfall time series during the EOC period for each site of interest from all snowfall (solid line, circle marks), snowfall during favorable 10 °C instability times (dashed line, square marks), and snowfall during favorable 13 °C instability times (dotted line, triangle marks).

Chapter 4

Lake-Effect Properties

Thus far what has been examined and discussed has been related to changes in overall snowfall and lake-effect snowfall in the Great Lakes and the changes in conditions that are responsible for these changes. In this chapter we now pivot to examining the changes in the properties and formation of lake-effect bands themselves, including their depth, updraft strength, and the environments in which they form. These properties contribute and influence the snowfall within lake-effect bands and are also important for the development of separated charge regions and thus the potential for lightning within lake-effect snowstorms.

4.1 Changes in Monthly Average Instability

The change in the monthly average temperature differential between 2 meters and 850 mb for each month during the cold season is shown in Figure 4.1. In the month of October (Figure 4.1a), we see a decrease in this temperature differential and therefore the instability across all of the lakes by EOC. This more stable background environment over the lakes will serve to inhibit lake-effect band formation. Moving to November (Figure 4.1b), a small increase in background instability is seen across Lake Superior and northern Lake Michigan with little to no changes across the rest of the Great Lakes. This change may support more lake-effect band formation over the northern Great Lakes, with no change in background support across the rest of the lakes. When

looking at the changes in the average background instability in December (Figure 4.1c) a widespread increase in temperature differential of about 2-3 °C is apparent over all of the Great Lakes. In January (Figure 4.1d), this widespread increase in temperature differential is again seen and is now greater (3-4 °C) across most of the lakes. Both of these months in the core winter season have the greatest changes in average background instability, allowing for much more support for lake-effect bands to form by EOC during these times. This large increase in average instability supports the results discussed earlier in Chapter 3 with favorable lake-effect snow events becoming more confined to and actually increasing in frequency during these months by EOC.

Looking at the month of February (Figure 4.1e), an increase in the average background instability is again seen over all of the lakes, now at a reduced magnitude compared to the previous months with increases of about 1-2 °C. These changes are still favorable for more lake-effect band development and is likely why in this month a slight increase in the number of favorable lake-effect occurrences is observed by EOC. Finally, changes in the March (Figure 4.1f) average background instability show unique spatial changes. A divide between the more northwestern lakes and the southeastern lakes is seen, with the northwestern portions of the lakes experiencing increased instability more than the southeastern lakes. Over Lake Superior and the northern parts of Lake Huron and Lake Michigan, these increases in average instability are actually slightly larger than those found previously in the month of February with increases of about 2-3 °C once more. However, despite this increase in average instability, a decrease in the number of favorable lake-effect occurrences is observed. This may be due to the increased instability signal not being consistent over all of the Great Lakes, as well as less occurrences of temperatures below freezing being present over the region in March which will serve to decrease favorable lake-effect snow occurrences.

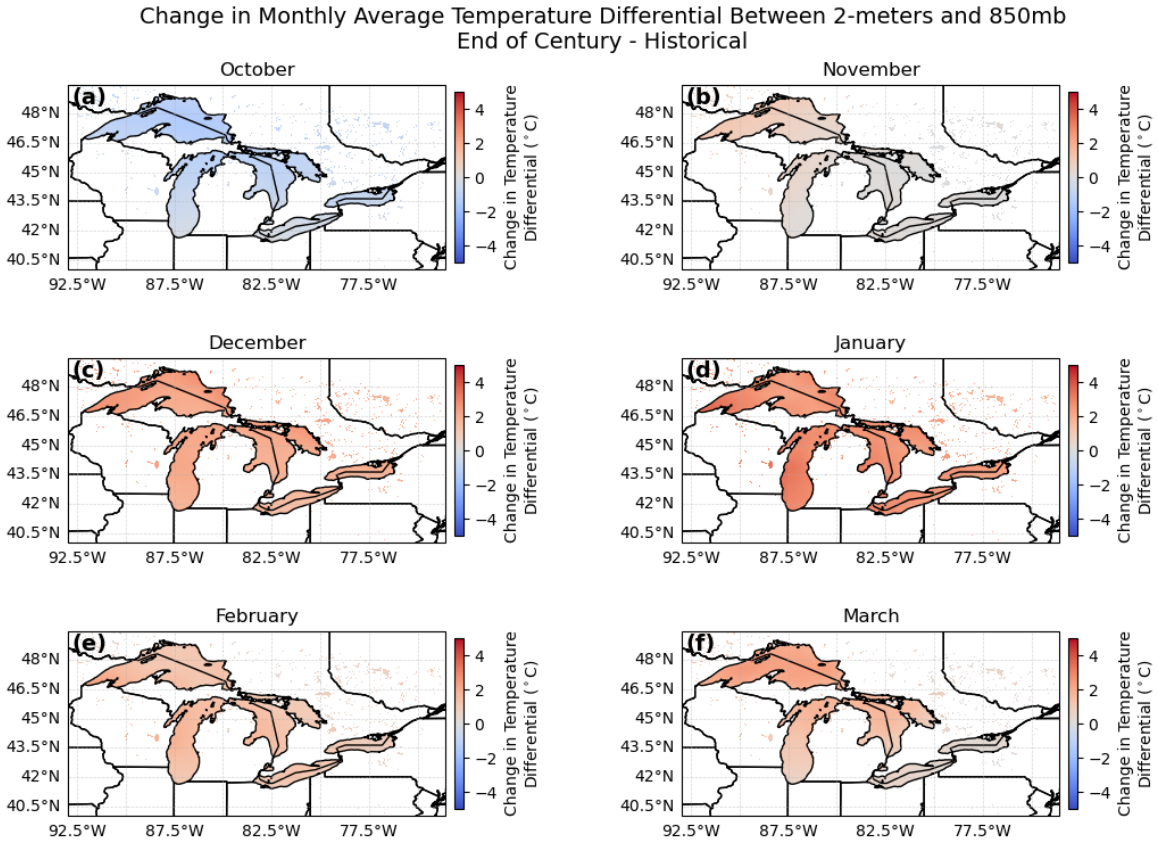

Figure 4.1: Changes in the monthly average temperature differential between 2 meters and 850 mb over the Great Lakes for each month during the cold season.

4.2 Changes in Lake-Effect Environments

Low-level instability is one ingredient in lake-effect band formation but does not fully explain how the environments that lake-effect bands form in are changing. In order to examine how the environments themselves are changing, composite soundings at each site of interest during favorable lake-effect times where snowfall was simulated at each site were plotted. These soundings are compared and shown in Figure 4.2 for 10 °C instability. It can be seen that each of these sites have different favorable wind directions, with some having nearly due westerly winds throughout the profile and others having northwesterly winds throughout. By EOC, these wind directions do not show much change. Some small increases and decreases in average wind speeds are seen, with slowing 1000 mb winds at Owen Sound for example. Each of the thermodynamic profiles show low-level instability with steeper lapse rates near the surface with near isothermal layers in the mid-levels. All of the temperature and moisture profiles exhibit a shift towards warmer temperature by EOC as would be expected in a warming climate. Although these temperature profiles are shifting towards warmer temperatures, it is apparent that the low-level average temperatures are warming slightly more than those in the mid to upper-levels. As a result, the low-level instability present within these lake-effect snow bands is increasing by EOC, matching the results discussed previously with increases in background instability and instability criterion occurrences in parts of the Great Lakes. The increase in low-level moisture and temperatures will also allow higher water contents within these lake-effect bands, potentially decreasing snow-to-liquid snowfall ratios with lake-effect snowfalls containing more liquid content as average near-surface temperatures reach closer to 0 °C.

Figure 4.3 shows the same composite soundings at each site of interest during favorable lake-effect times with simulated snowfall but for the 13 °C instability criteria.

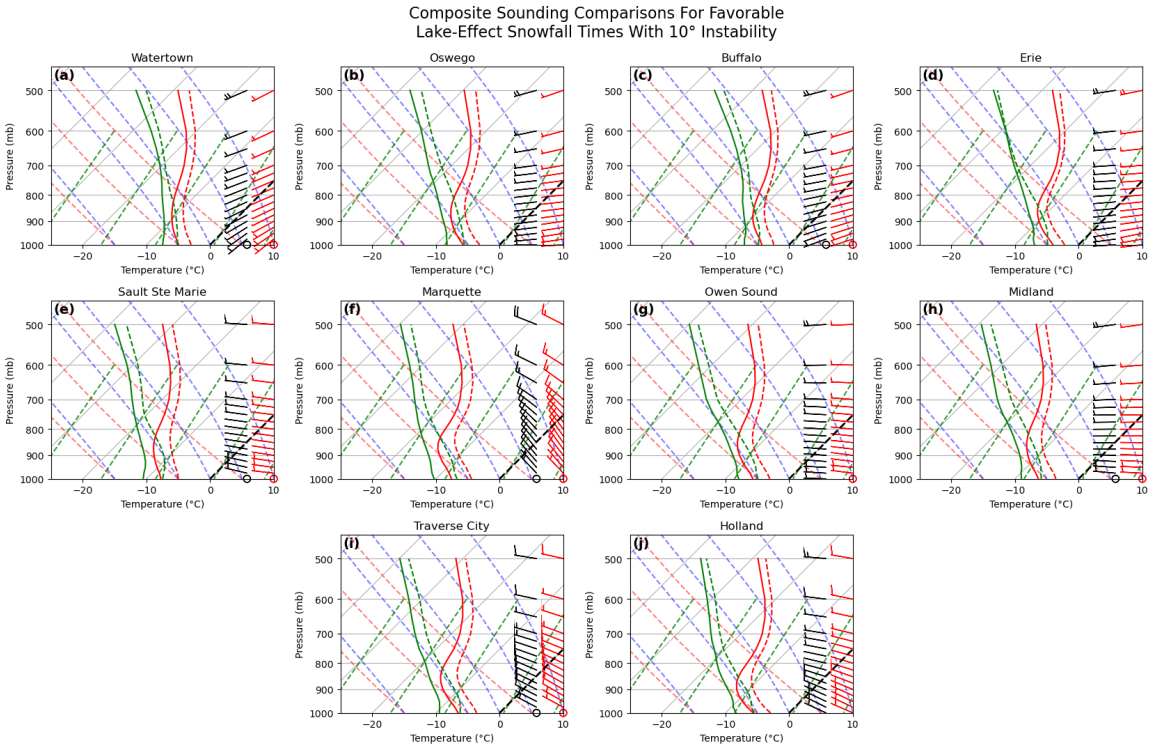

Figure 4.2: Composite soundings for favorable 10 °C instability snowfall times where at least 0.1 in (2.54 mm) of 6-hourly snowfall was recorded at each site of interest. Red and green solid (dashed) lines show the historical (EOC) temperature and dew point profile, respectively. Black (red) wind barbs show the Historical (EOC) wind profile. Sites off Lake Ontario are shown in panels a and b, off Lake Erie shown in panels c and d, off Lake Superior in panels e and f, off Lake Huron in panels g and h, and off Lake Michigan in panels i and j.

Once again, little to no changes are apparent in the wind profile by EOC, however the wind profiles for each site during 13 °C favorable times are slightly more backed (counter-clockwise turning) compared to those for the 10 °C favorable times (Figure 4.2). The thermodynamic profiles in these cases show larger low-level lapse rates towards the surface than in the 10 °C composite soundings and an even more apparent near-isothermal layer between 700 and 800 mb. As was seen previously with the 10 °C composite soundings, nearly all the temperature and moisture profiles shift towards warmer temperatures by EOC, with near-surface temperatures in both periods being colder than those found in each respective period in the 10 °C soundings. The greatest increases in average dew point and temperature are found in the low levels of the profile and are increasing more than those in the mid to upper-levels by EOC. The only place where this does not occur is in Watertown, NY where the temperature profile remains nearly unchanged and the moisture profile becomes slightly drier. With lower-level temperatures and moisture increasing more than the rest of the profile, the increase in low-level instability by EOC is seen once again with a greater increase than in the 10 °C favorable times.

The previous two figures examined the composite soundings of favorable lake-effect conditions with snowfall at each of the sites of interest. However, these sites are all on land and therefore do not represent the true environment lake-effect snow bands form in and how they may change in a warming climate. To address this issue, composite soundings during favorable lake-effect times with snowfall 50 km upwind of each site were plotted and examined in order to better capture changes in the over-lake environments. The sites of these upwind locations along with their associated on-land sites of interest are shown in Figure 4.4. These new over-lake composite soundings for favorable lake-effect snowfall times with 10 °C instability are shown in Figure 4.5. One difference

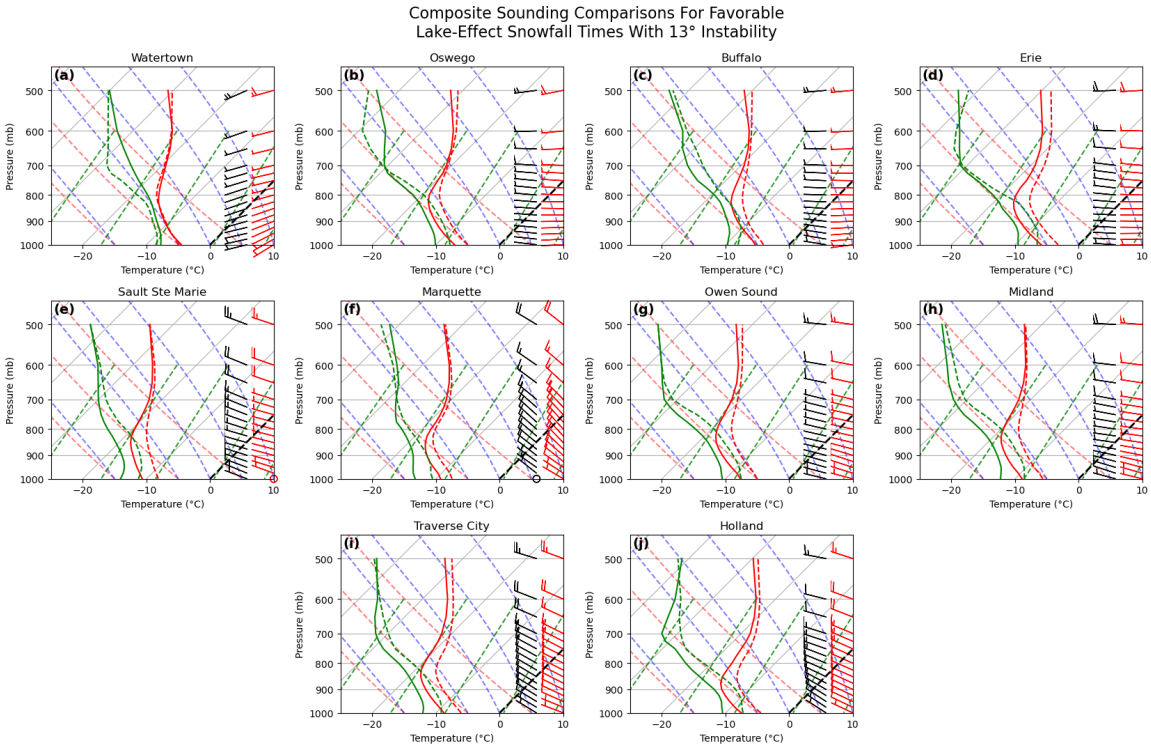

Figure 4.3: Composite soundings for favorable 13 °C instability snowfall times where at least 0.1 in (2.54 mm) of 6-hourly snowfall was recorded at each site of interest. Red and green solid (dashed) lines show the historical (EOC) temperature and dew point profile, respectively. Black (red) wind barbs show the Historical (EOC) wind profile. Sites off Lake Ontario are shown in panels a and b, off Lake Erie shown in panels c and d, off Lake Superior in panels e and f, off Lake Huron in panels g and h, and off Lake Michigan in panels i and j.

between the over-lake sites and the on-land sites is the slight increase in near-surface winds. This is to be expected when examining a point over water as opposed to land, as surface roughness is less over water and allows for wind speeds to be greater and unimpeded. Most of the over-lake profiles remain roughly the same compared to those at the on-land sites of interest, although the temperatures and dew points towards the surface are shifted towards warmer temperatures due to the presence of the warmer lake waters. This results in a sharpening of the low-level lapse rates closer to the dry adiabatic lapse rate, and increased instability in the area where these lake-effect bands form compared to where they are impacting. The change in the upwind profiles between periods is also very similar to the changes observed in the on-land profiles, supporting that no major differences in the changes by EOC are taking place between over-lake and on-land points during favorable lake-effect times.

Figure 4.6 shows the composite soundings for favorable lake-effect snowfall times with 13 °C instability at the upwind locations of each site. An even greater increase in near-surface winds at the over-lake sites is seen in these composites, with many 1000-mb average winds increasing by about 5 knots compared to the on-land sites. In contrast to the 10 °C composite soundings, there are smaller increases in low-level temperatures and moisture between the on-land sites of interest and the over-lake sites. Many over-lake sites, including Watertown, Buffalo, and Holland, in fact have their near-surface temperatures stay the same or even decrease slightly compared to their respective on-land sites. This may be a result of these higher instability events only occurring during cold air outbreaks in which the near surface air is very cold by EOC, as warming temperatures make the instability condition harder to reach in these regions. There are a few exceptions to this, with sites upwind of Sault Ste Marie, Owen Sound, and Midland showing an increase in near-surface temperatures and moisture

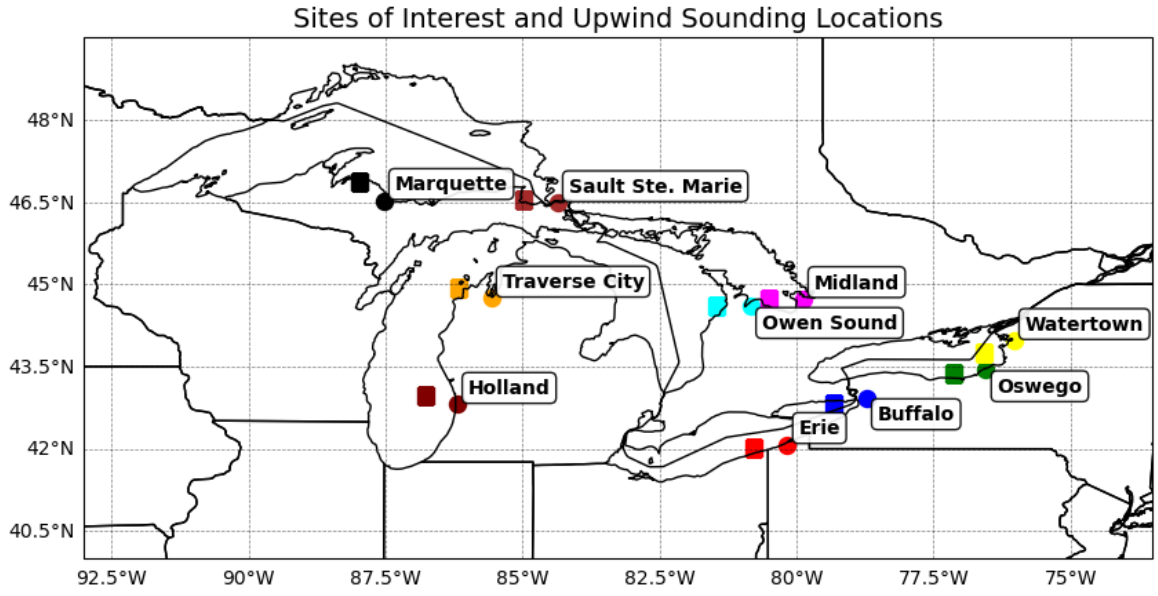

Figure 4.4: Map of the domain highlighting the sites of interest examined in this study as well as the locations of their upwind composite sounding sites shown by the square markers with colors corresponding to each respective downwind site.

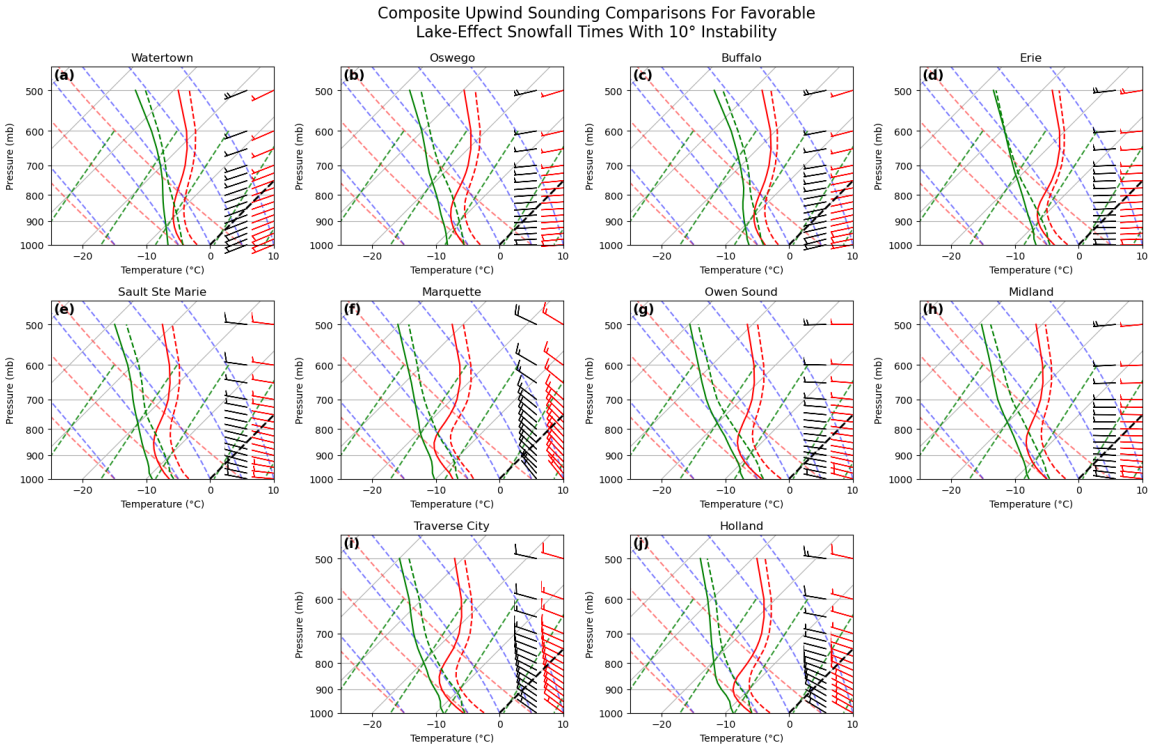

Figure 4.5: Same as Figure 4.2 but for points 50 km upstream of each site of interest.

compared to the on-land sites. These over-lake sites again show the increase in lower-level instability and lapse rates compared to their on-land counterparts due to the presence of the warmer lake waters, showing a more unstable environment for lake-effect bands to form in over the lakes as expected. When comparing the over-lake composite soundings between periods, changes very similar to those shown in the on-land composite soundings (Figure 4.3) are observed.

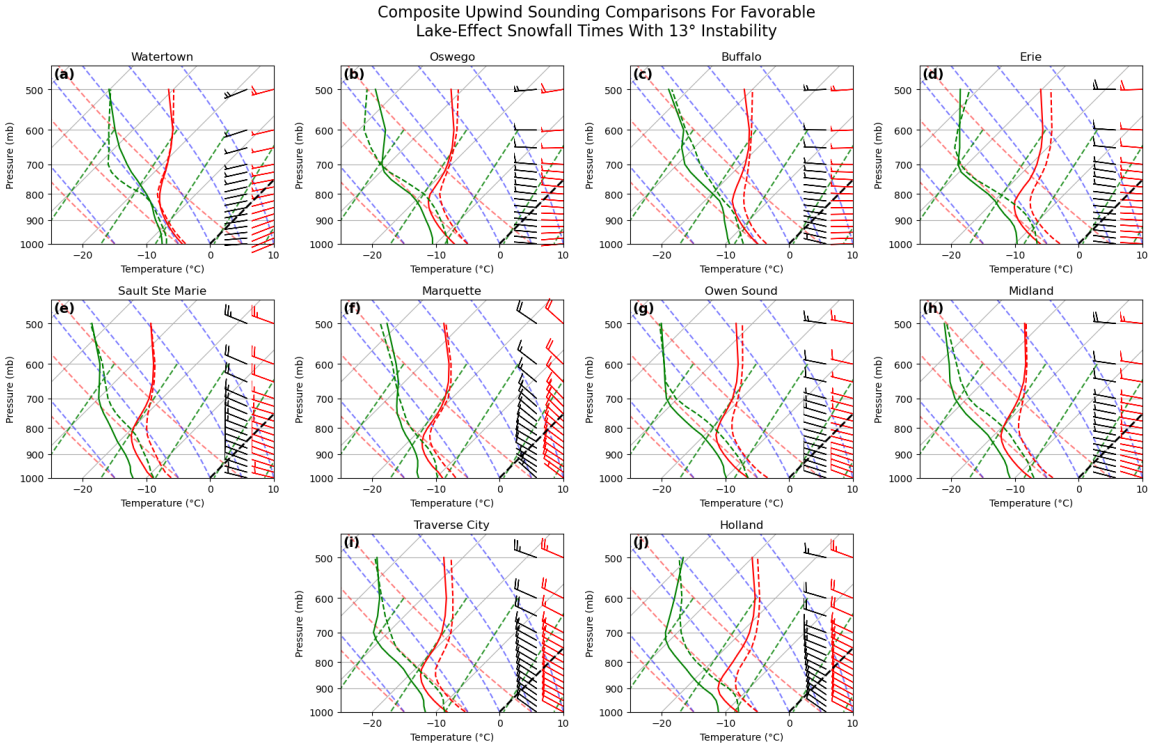

Figure 4.6: Same as Figure 4.3 but for points 50 km upstream of each site of interest.

4.3 Changes in Electrification Properties of Lake-Effect Snow

Up to this point, it has been shown that overall monthly average instability during the cold season and the instability of the environment during favorable lake-effect snowfall times are expected to increase by EOC. This comes as a result of steepening low-level lapse rates due to larger increases in both temperature and moisture near the surface compared to the rest of the environment. With these expected increases in the instability available to lake-effect snow bands during their formation and propagation, changes in the properties of lake-effect bands, such as their depth and the strength of their updrafts can be expected as well. To examine these properties the average echo top height and average maximum updraft speed were calculated. Using the average

echo top height of lake-effect snow bands will assist in giving a proxy of the average depth of lake-effect snow bands. Likewise the average maximum updraft speed allows assessment of the strength of the updrafts in these lake-effect snow bands.

The change in the average echo top height and the relative change in the average maximum updraft speed during favorable lake-effect snowfall times with 10 °C instability are shown in Figure 4.7. By EOC the average echo top height of lake-effect snow bands is expected to increase over nearly all of the lakes. Significant increases in average echo top height are seen over eastern Lake Ontario, northern Lake Michigan, and most of Lake Huron and Lake Superior. Over Lake Superior, some average echo top height increases are reaching nearly 300 meters, with significant increases over Lake Huron of around 100 to 150 meters. When examining the relative change in average maximum updraft speed, the highest increases are clearly seen over the Upper Great Lakes, such as Lake Superior, Lake Huron, and the northern portion of Lake Michigan. These areas of highest increases are coincident with the regions of the highest increases in average echo top height, with relative average increases over Lake Superior approaching 50%. The areas of highest increases match up well with regions where increases in the average favorable lake-effect 6-hourly snowfall and average favorable lake-effect event total snowfall were found earlier in Chapter 3. Other small increases are observed over Lake Erie and Lake Ontario with little to no change in the average maximum updraft speed over the rest of the domain.

Figure 4.8 shows the changes in average echo top height and relative changes in average maximum updraft speed during favorable lake-effect snowfall times but with the 13 °C instability criteria. During these more intense events significant changes in the average echo top height are more confined to the snowbelts off Lake Superior and Lake Huron with some scattered significant increases along the west coast of Michigan. Over

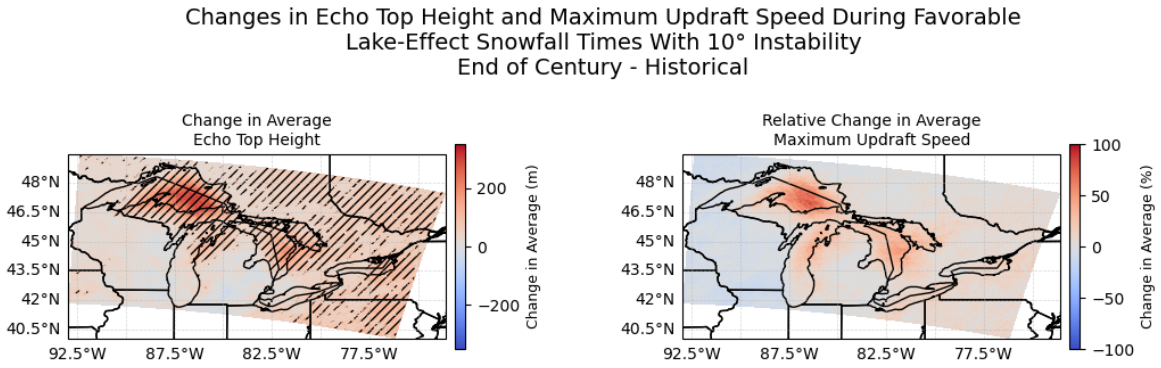

Figure 4.7: Changes between periods (EOC - Historical) in the average echo top height in meters (left) and the relative change in the average maximum updraft speed in percent (right) during favorable 10 °C instability times. Hatching signifies significant changes at the 99% confidence level using the bootstrapping approach summarized in the Data and Methods Chapter 2.

Lake Superior and Lake Huron, average echo top heights are expected to increase by around 400 meters, nearly half a kilometer. The relative changes in average maximum updraft speed are spatially similar to those found in the 10 °C favorable times but with larger magnitudes. Co-located once again with the significant and highest increases in average echo top height, relative changes in the average maximum updraft speed are reaching nearly 100% by EOC over Lake Superior and Lake Huron. Other smaller relative average increases are also seen over Lake Erie and Lake Ontario that were not apparent in the 10 °C instability favorable lake-effect snowfall times.

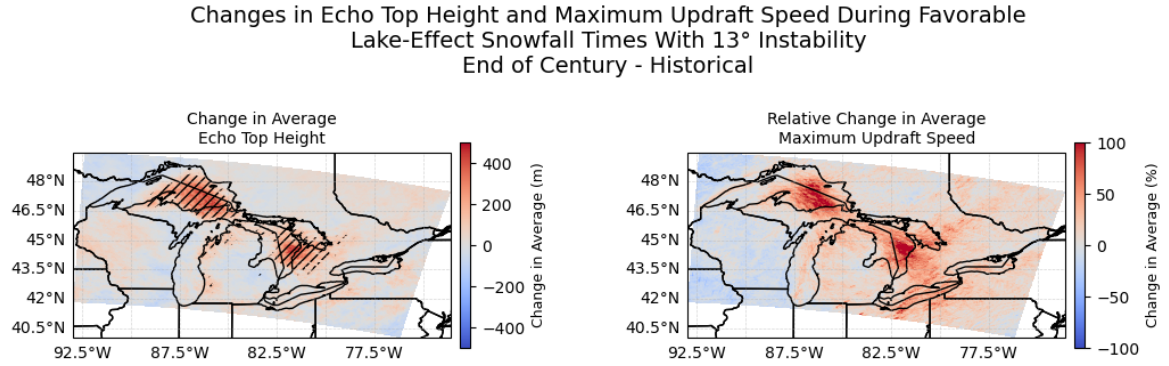

Figure 4.8: Changes between periods (EOC - Historical) in the average echo top height in meters (left) and the relative change in the average maximum updraft speed in percent (right) during favorable 13 °C instability times. Hatching signifies significant changes at the 99% confidence level using the bootstrapping approach summarized in the Data and Methods Chapter 2.

Chapter 5

Summary and Conclusions

5.1 Summary

In this study, dynamically downscaled GCM simulations were analyzed to examine changes in lake-effect snowfall across the Great Lakes in the context of a changing climate. A unique and novel aspect of this study is the use of high-resolution dynamically downscaled data over the entirety of the Great Lakes region, which can better resolve convective features associated with lake-effect snow compared with prior studies. This study is also the first to exhibit quantitative changes in lake-effect snow due to a warming climate across all of the Great Lakes, and to show expected changes both temporally and spatially across the region. A unique opportunity is then provided to expand on prior studies and analyze changes in the precipitation rate and occurrences with increased accuracy and confidence. Atmospheric parameters conducive for lake-effect snow were also examined to provide context for why these changes may take place. In a warming climate, this study revealed a decrease in seasonal snowfall across much of the Great Lakes region, especially in the transition season of SON and MAM. This finding is consistent with snowfall decreases found in previous studies (Ashley et al. 2020; Baijnath-Rodino et al. 2018; Hartnett et al. 2014). However, seasonal snowfall remains near constant or even increases in prominent lake-effect belts due to lake-effect snowfall. This result is similar to those found in Burnett et al. (2003).

High-end snowfall accumulations in lake-effect-prone regions showed increased snowfall by EOC, especially off of Lake Superior and Lake Huron.

To isolate snowfall change to those only derived from changes in lake-effect snow events, criteria adapted from Kunkel et al. (2002) were used to identify favorable times for lake-effect snow. A domain-wide decrease in the occurrence of favorable temperatures and increase in favorable 10 °C instability drive the overall changes in the occurrence of favorable lake-effect conditions by EOC. Favorable lake-effect conditions are also more confined to the core winter season (DJF) by EOC. When these same conditions were tested with 13 °C instability, similar results were found with a smaller sample size of events. The instability criterion was the main driver in overall changes in favorable lake-effect condition occurrences; however, the occurrence of favorable 13 °C instability and all conditions together was shown to decrease only over Lake Ontario by EOC. Convergence of the 10-m wind during these favorable times was also shown to increase even more over the prevailing downwind shores of each of the lakes. Overall, these results indicate that in a warming climate, lake-effect snow may become less common over the lower Great Lakes, such as Lake Ontario and Lake Erie, but more common across much of Lake Superior and parts of Lake Huron and Lake Michigan, with a temporal shift toward DJF.

Higher-end lake-effect snowfall amounts during favorable 10 °C instability times are also found to increase downwind of Lakes Superior, Huron, and Michigan with the most extreme increases of 50 mm/6hr or greater. During favorable 13 °C instability times, these increases are more confined to downwind of Lake Superior and Lake Huron with the largest increases upwards of 100 mm/6hr corresponding to an average increase of around 0.67 inches per hour. Such increases in snowfall may lead to dangerous conditions and disrupt infrastructure and daily life in areas that previously may have only rarely experienced such intense snowfall. When comparing the average 6-hourly

snowfall over all times and those only during favorable 10 °C instability lake-effect conditions, it is found that lake-effect snow is expected to maintain its average intensity or significantly increase in the lake-effect belts of Lake Superior, Lake Huron, and Lake Michigan. Meanwhile, areas outside of the lake-effect belts experience large decreases in average snowfall intensity due to decreases in non-lake-effect snow events. During favorable 13 °C instability favorable conditions, significant increases in the average 6-hourly snowfall intensity are seen in these same regions and are larger, with significant increases now also seen to the southeast of Lake Erie and to the east of Lake Ontario.

When classified into lake-effect snow events, i.e., continuous periods with favorable 10 °C instability lake-effect snow conditions, fewer lake-effect snowfall events are expected by EOC. However, the average total snowfall from each of these events is expected to remain the same or even increase, e.g., off of Lake Huron and Lake Superior. These events may also experience a slight increase in duration and exhibit much higher average event total snowfalls in the most extreme events. Similar results are found when examining classified lake-effect snow events with favorable 13 °C instability lake-effect snow conditions, with average snowfall totals from these events now increasing off of Lake Erie and Lake Ontario as well. Although less events are included in the 13 °C lake-effect event duration distributions, an even greater increase in duration by EOC is seen with these lake-effect snow events.

Each of the sites of interest in the domain located in prominent lake-effect snow belts were also examined for the amount of snowfall each receives in every season. The total snowfalls were separated between all snowfalls and snowfalls during the favorable lake-effect times with 10 °C and 13 °C instability. In a warming world, seasonal snowfall totals were shown to decrease at the sites off Lake Erie, Lake Ontario, and Lake Michigan while remaining the same or increasing slightly off Lake Huron and Lake Superior. The percentage of total seasonal snowfall contributed during favorable

lake-effect times was also shown to increase at all sites. By EOC, snowfall during favorable 10 °C instability lake-effect times comprised 50% or more of the total seasonal snowfall at nearly all the sites of interest. This analysis leads to the conclusion that in a warming world snowfall from synoptic systems will lessen across the Great Lakes allowing lake-effect snow to become the main contributor to snowfall and the snowfall budget in the region. This can have major implications as lake-effect snow often occurs over small regions and is not widespread in nature, which may lead to regions not retaining constant yearly snowfall that is needed for runoff and water resources.

In order to examine other impacts and properties of lake-effect snow bands that were not tied solely to snowfall, properties related to the electrification of lake-effect snow bands and the occurrence of thundersnow in these bands were also analyzed. Within the core winter months of DJF, monthly average low-level instability increased by anywhere from 1-3 °C, consistent with Baijnath-Rodino et al. (2018), significant changes given only a 13 °C temperature differential is needed in the low-levels in order to produce pure lake-effect snow (Niziol et al. 1995). These increases in average low-level instability may also contribute to deeper lake-effect snow bands with stronger updrafts, both of which can contribute to increases in the electrification of this phenomenon. In the transition months of October or November, the average monthly instability had negligible changes or was decreasing which serves to actively hamper lake-effect snow formation chances. These results again connect well to the temporal changes that were seen in the occurrence of favorable lake-effect conditions, with favorable occurrences increasing in the core winter season and decreasing in the transition season in a warming world.

By analyzing composite soundings of favorable lake-effect snowfall occurrences at each of the sites of interest, changes in lake-effect environments in a warming world could be seen. The average wind profiles for favorable lake-effect snow occurrences at

each site remained qualitatively the same as expected due to certain wind directions and fetches being necessary for each site to be impacted. The average environments during both favorable 10 °C and 13 °C instability lake-effect snowfall times exhibited a shift in the temperature and moisture profiles towards warmer temperatures by EOC. In the low-levels of the environments, these shifts were the greatest and contributed to higher low-level lapse rates and instability for lake-effect snow bands to form in and make use of. When examining over-lake sites upwind of each on-land site of interest to better capture changes in the average over-lake environments, near-surface temperatures and dew points are shown to be greater than at the on-land sites. As expected, this results in stronger lapse rates and greater instability over the lakes where lake-effect snow bands form, which increase even more by EOC at most of the over-lake sites. This is consistent with previous findings from Suriano (2019) where increasing boundary layer instabilities were seen in multiple lake-effect synoptic types from 1950 to 1979. Given the higher moisture and instability available to lake-effect bands in the future, one can expect deeper lake-effect bands and stronger updrafts again may increase electrification potential.

The changes in the average echo top height and relative average maximum updraft speed are then examined to quantify changes in band structure and electrification potential. By EOC, average echo top heights are expected to increase significantly across nearly all of the lakes, with the highest increases near 0.5 km over Lake Superior and Lake Huron. As shown in previous studies (Reinking et al. 1993; Steiger et al. 2013; Minder et al. 2015), the typical echo top heights of LLAP lake-effect bands over Lake Ontario are between 2-4 km, with some reaching around 5 km. Likewise, the largest relative changes in average maximum updraft speed are found in these areas with the averages during favorable 13 °C instability lake-effect times increasing by nearly 100% by EOC. Over Lake Ontario, it has been shown that lake-effect band updraft speeds are

usually in the range of 1-5 m/s, with maximum speeds up to 10 m/s (Minder et al. 2015; Steiger et al. 2018). Although these values for echo top heights and updraft speeds have been found for deeper and singular lake-effect bands off the eastern Great Lakes, they are likely representative, albeit at lesser magnitudes, for lake-effect bands that form over Lake Superior and Lake Huron. Even so, the increases observed in the data suggest significant deepening and increases in updraft strength for lake-effect bands off these lakes. With these increases there likely will be increases in electrification off Lake Huron and Lake Superior in particular as well as increases in lake-effect thundersnow occurrences, which may shift the wintertime lightning climatology across the Great Lakes found by Letcher and Steiger (2010).

Lake-effect snow in the Great Lakes is expected to change in a warming world. From this study, we see that the most profound impacts and changes are likely to occur off Lake Superio and Lake Huron, with lesser changes present over Lake Michigan. These changes will include increases in total snowfall from lake-effect snow events as well as increases in the intensity of these bands. By EOC lake-effect snowfall makes up the majority of total seasonal snowfall for locations in prominent lake-effect snow belts, changing the snowfall climatology of these locations. This may reduce the confidence in certain areas receiving their normal snowfall amounts within a season, due to lake-effect snow's more inherent unpredictability and its smaller spatial footprint. More profound lake-effect snow in these regions is likely in part caused by warmer lake waters, less often/pronounced lake ice cover, and increases in surface temperatures closer to freezing during the cold season. These changes in ice cover and warmer lake waters are also contributing to increased instability for lake-effect snow bands to make use of. With the increased instability deeper and stronger lake-effect snow bands can be expected, perhaps with more electrification and thundersnow occurrences across the Great Lakes.

5.2 Future Steps and Analysis

This study went in depth into multiple aspects of lake-effect snow and how they may change in a warming climate under the IPCC's RCP8.5 emission scenario. However, many of the methods and analyses performed in this study could be done differently to answer different questions or to explore different hypotheses. For example, if the data were available from this simulation it would serve well to examine these same changes under a different IPCC RCP scenario between the historical period and the middle of the century instead of the end of century. This would allow conclusions to be drawn about changes throughout the century and between emission scenarios, such as if they are exponential or linear in nature. Performing these analyses once more with hourly temporal resolution could perhaps allow more extreme changes in lake-effect snow intensity to be seen. This is because lake-effect snow is a mesoscale feature that can change quickly over shorter timescales then what was examined in this study, as 6-hourly temporal resolution was chosen to minimize time and computational expenses.

If available, utilizing lake surface temperatures instead of 2-m temperatures in our low-level instability calculation would provide a more accurate depiction of instability changes across the Great Lakes. It would also allow more accurate classification of favorable lake-effect snow conditions for both instabilities while possibly capturing lake-effect snow occurrences that may have been missed and restricting any occurrences that may have been mistakenly selected due to the difference in calculation. There are many other avenues in which this research can be further taken. One could choose to examine whether the inland extent of lake-effect snow is changing due to warming temperatures and increased instability by creating an index or threshold for inland snow extent. With warming temperatures, it may also serve well to examine sensitivity of lake-effect snowfall amounts to already existing ground snow pack. This existing snow

pack could assist in providing surface temperatures cold enough for snow in a world where below freezing temperatures become less common. Analysis of the snow pack could also extend to changes in rain on snow events in the region, which can lead to flooding via heavy rainfall and large amounts of snow melt simultaneously.

One step of future analysis that was commenced during this study was examining the 15-minute model output composite reflectivity of different lake-effect bands to identify possible changes in the frequency of each band type in a warming climate. The details on each of these lake-effect types are covered back in Chapter 1. From the list of favorable 10 °C instability lake-effect times, a random time was chosen. The composite reflectivity at the randomly selected time and the two hours before and after this time were then plotted. For each of these plots it was then designated whether the reflectivity signature resembled pure lake-effect precipitation, a hybrid of lake-effect and synoptic precipitation, or non-lake-effect precipitation. The resulting reflectivity images were then grayscaled and organized into folders containing the classifications of precipitation discussed previously. Some examples of the final grayscaled images are shown in Figure 5.1, with Figure 5.1a showing a pure lake-effect event, Figure 5.1b showing a hybrid of lake-effect and non-lake-effect precipitation, and Figure 5.1c being classified as non lake-effect precipitation. This process was done to produce enough samples in each classification for a machine learning model to learn to identify lake-effect bands on its own based on composite reflectivity images from the simulation. The end goal was to have the model classify each of the 5 lake-effect snow band types discussed by Niziol et al. (1995) and potentially give heat maps of where and when these bands occurred in both periods. From these results comparisons could then be made in order to see potential changes in lake-effect snow band structure and placement in a warming climate.

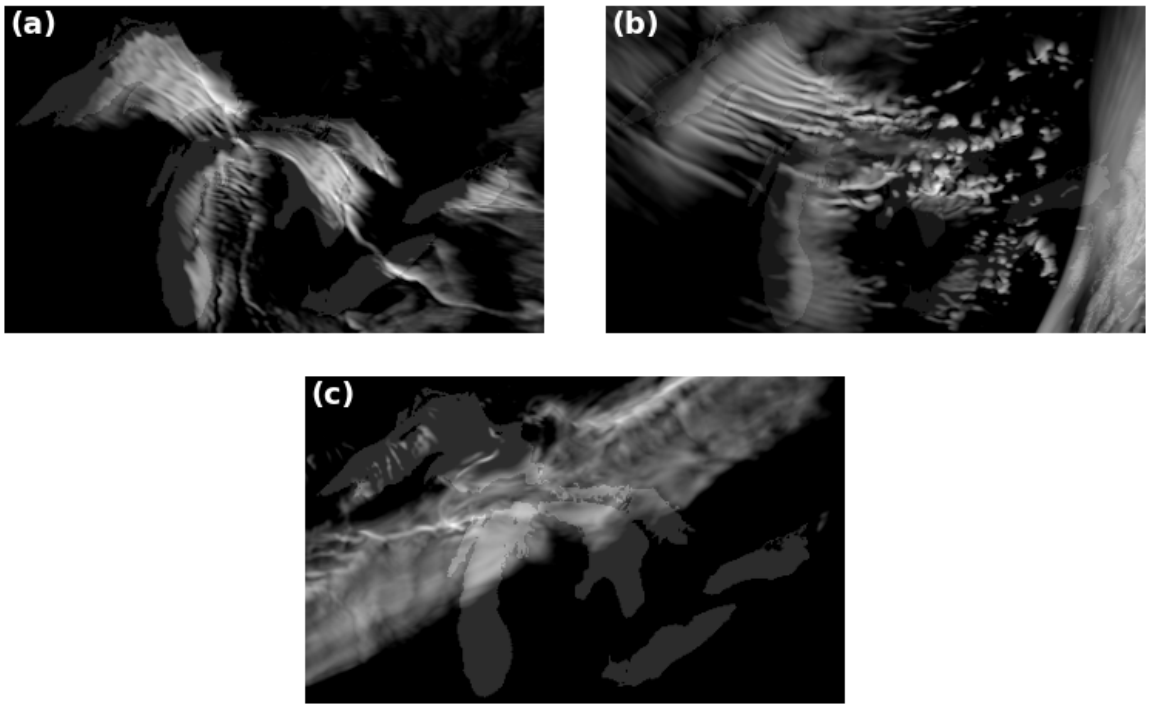

Figure 5.1: Grayscaled composite reflectivity imagery designated as (a) pure lake-effect precipitation, (b) a hybrid of lake-effect and non-lake-effect precipitation, (c) non-lake-effect precipitation.

This analysis did not fully come to fruition as it is beyond the scope of the current work, but the random selection of favorable 10 °C instability lake-effect times allowed for strengths of the simulation to be seen in the context of this research. From the composite reflectivity images it was apparent that the simulation was able to resolve and predict all five types of lake-effect snow bands, with each being found at multiple different times. An example of the model simulating a Type I lake-effect band is shown in Figure 5.2, a Type II lake-effect band is shown in Figure 5.3, a Type III band is shown in Figure 5.4, an impressive Type IV band is shown in Figure 5.5, and finally a Type V mesovortex lake-effect band is in Figure 5.6. With further analysis not shown in this thesis the model simulation was also able to resolve fine-scale shear zones near

these simulated lake-effect bands that are crucial in lake-effect snow band formation and maintenance.

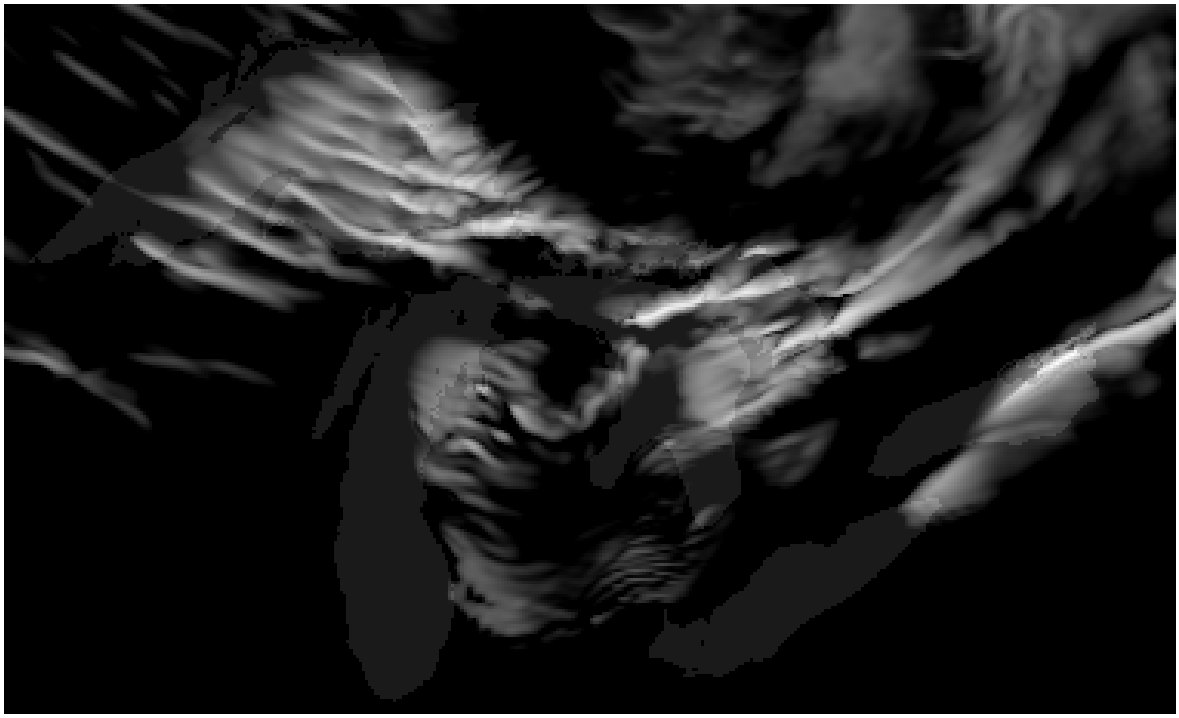

Figure 5.2: Grayscaled composite reflectivity imagery from a random favorable 10 °C instability lake-effect snow time. In this instance, a Type I long-lake-axis-parallel (LLAP) lake-effect snow band is simulated over eastern Lake Ontario.

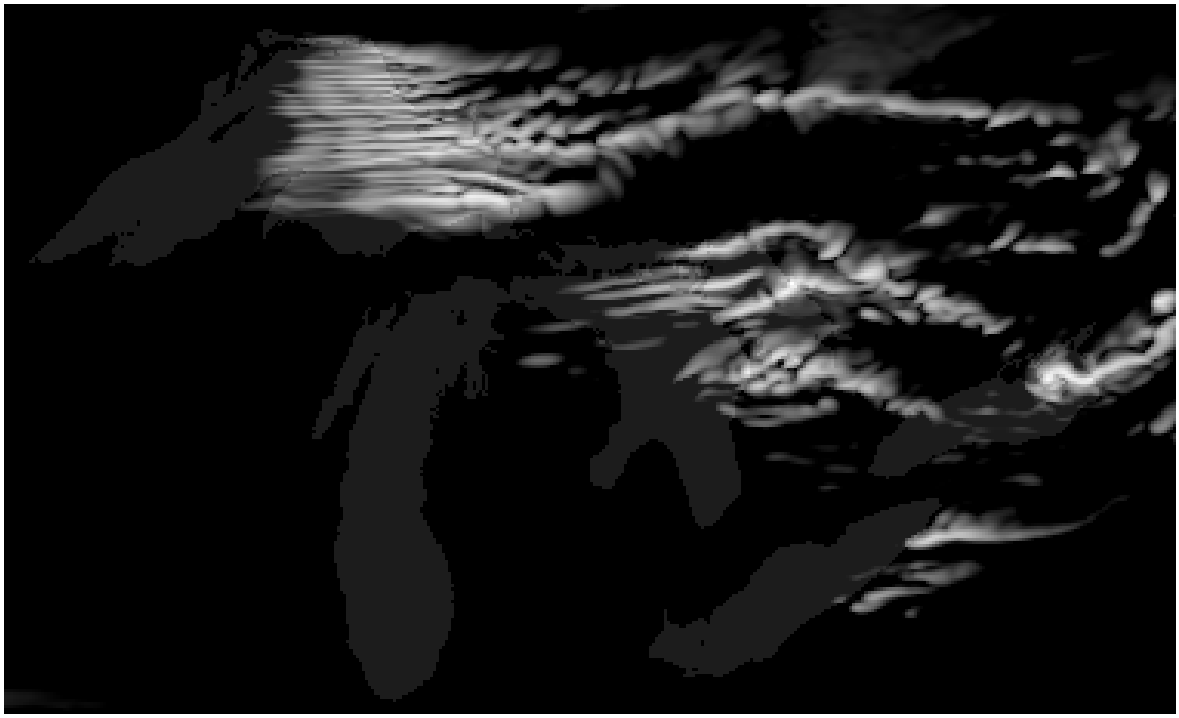

Figure 5.3: Grayscaled composite reflectivity imagery from a random favorable 10 °C instability lake-effect snow time. In this instance, a Type II short lake-axis lake-effect snow band is simulated over Lake Superior and Lake Huron.

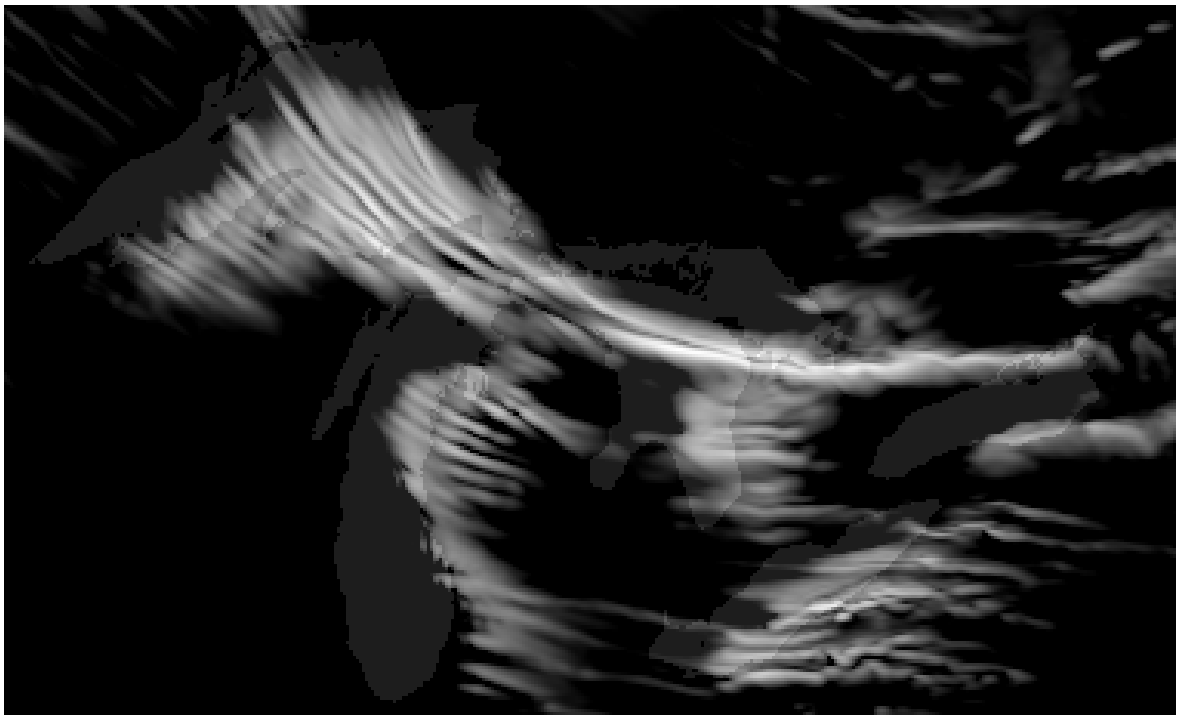

Figure 5.4: Grayscaled composite reflectivity imagery from a random favorable 10 °C instability lake-effect snow time. In this instance, a Type III hybrid lake-effect snow band is simulated over Lake Superior downwind over Lake Huron reaching to northern Lake Ontario.

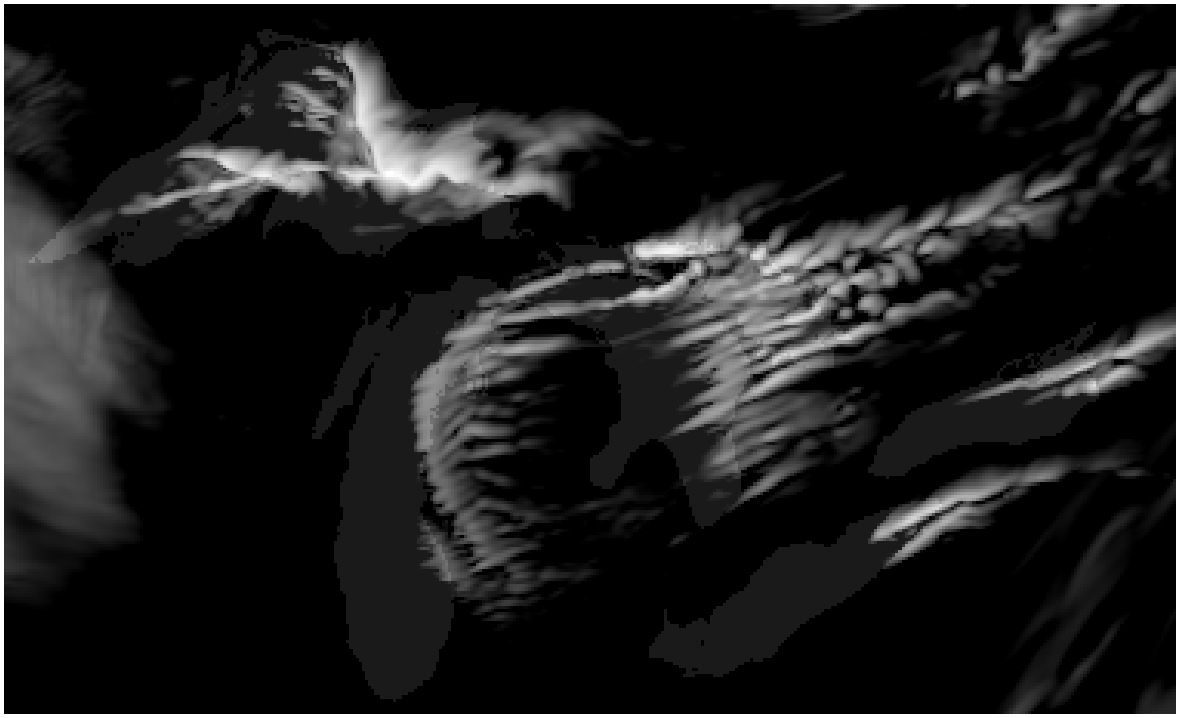

Figure 5.5: Grayscaled composite reflectivity imagery from a random favorable 10 °C instability lake-effect snow time. In this instance, a Type IV near-shore wind parallel lake-effect snow band is simulated over eastern Lake Superior.

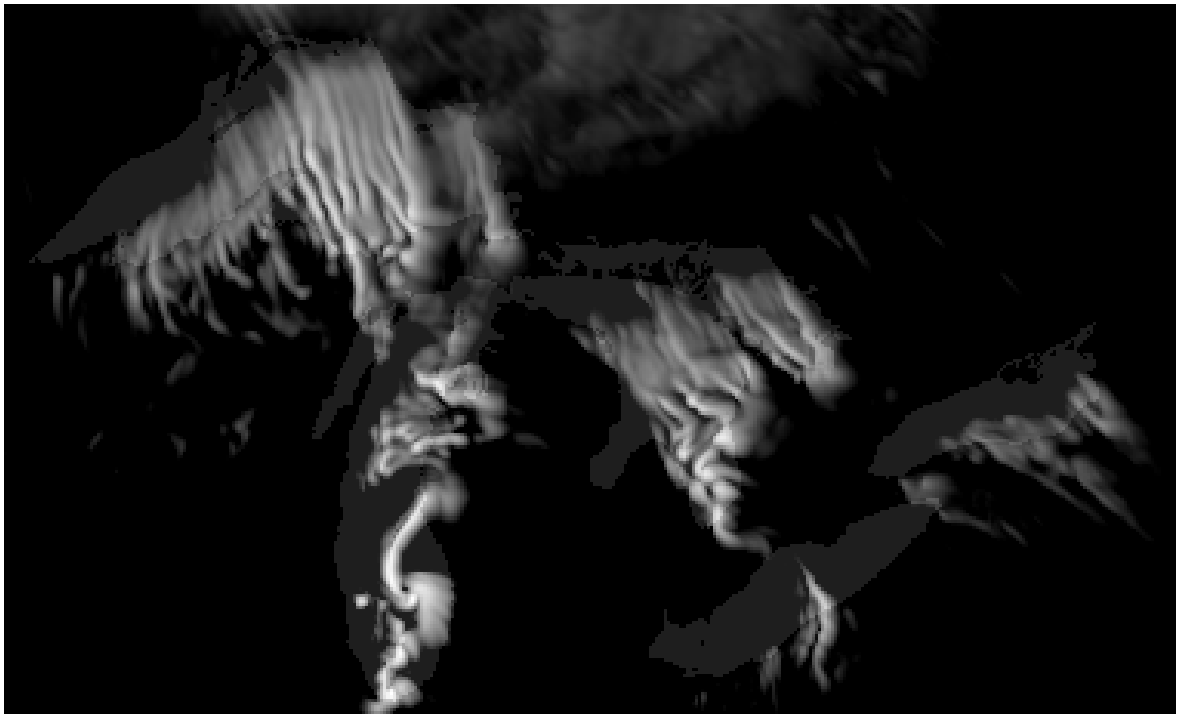

Figure 5.6: Grayscaled composite reflectivity imagery from a random favorable 10 °C instability lake-effect snow time. In this instance, a Type V mesovortex lake-effect snow band is simulated over southern Lake Michigan.

Reference List

Ashley, W. S., A. M. Haberlie, and V. A. Gensini, 2020: Reduced frequency and size of late-twenty-first-century snowstorms over north america. *Nature Climate Change*, **10**, 539–544, https://doi.org/10.1038/s41558-020-0774-4.

Assel, R., K. Cronk, and D. Norton, 2003: Recent trends in laurentian great lakes ice cover. *Climatic Change*, **57 (1)**, 185–204, https://doi.org/10.1023/A:1022140604052.

Baijnath-Rodino, J. A., C. R. Duguay, and E. LeDrew, 2018: Climatological trends of snowfall over the laurentian great lakes basin. *International Journal of Climatology*, **38 (10)**, 3942–3962, https://doi.org/https://doi.org/10.1002/joc.5546.

Bard, L., and D. A. R. Kristovich, 2012: Trend reversal in lake michigan contribution to snowfall. *Journal of Applied Meteorology and Climatology*, **51 (11)**, 2038–2046, https://doi.org/10.1175/JAMC-D-12-064.1.

Bruyère, C. L., J. M. Done, G. J. Holland, and S. Fredrick, 2014: Bias corrections of global models for regional climate simulations of high-impact weather. *Climate Dynamics*, **43 (7)**, 1847–1856, https://doi.org/10.1007/s00382-013-2011-6.

Burnett, A. W., M. E. Kirby, H. T. Mullins, and W. P. Patterson, 2003: Increasing great lake–effect snowfall during the twentieth century: A regional response to global warming? *Journal of Climate*, **16 (21)**, 3535–3542, https://doi.org/10.1175/1520-0442(2003)016⟨3535:IGLSDT⟩2.0.CO;2.

Cannon, D., J. Wang, A. Fujisaki-Manome, J. Kessler, S. Ruberg, and S. Constant, 2024: Investigating multidecadal trends in ice cover and subsurface temperatures in the laurentian great lakes using a coupled hydrodynamic–ice model. *Journal of Climate*, **37 (4)**, 1249–1276, https://doi.org/10.1175/JCLI-D-23-0092.1.

Efron, B., and R. J. Tibshirani, 1994: *An Introduction to the Bootstrap*. Chapman and Hall, https://doi.org/https://doi.org/10.1201/9780429246593.

Environmental Protection Agency, 2025: Great lakes facts and figures. URL https://www.epa.gov/greatlakes/great-lakes-facts-and-figures, accessed May 29th, 2025.

Forbes, G. S., and J. H. Merritt, 1984: Mesoscale vortices over the great lakes in wintertime. *Monthly Weather Review*, **112 (2)**, 377–381, https://doi.org/10.1175/1520-0493(1984)112⟨0377:MVOTGL⟩2.0.CO;2.

Gensini, V. A., A. M. Haberlie, and A. S. Walker, 2022: Convection-permitting simulations of historical and possible future climate over the contiguous united states. *Climate Dynamics*, **60**, 109–126, https://doi.org/10.1007/s00382-022-06306-0.

Hanrahan, J., J. Langlois, L. Cornell, H. Huang, J. M. Winter, P. J. Clemins, B. Beckage, and C. Bruyère, 2021: Examining the impacts of great lakes temperature perturbations on simulated precipitation in the northeastern united states. *Journal of Applied Meteorology and Climatology*, **60 (7)**, 935–949, https://doi.org/10.1175/JAMC-D-20-0169.1.

Hartnett, J. J., J. M. Collins, M. A. Baxter, and D. P. Chambers, 2014: Spatiotemporal snowfall trends in central new york. *Journal of Applied Meteorology and Climatology*, **53 (12)**, 2685–2697, https://doi.org/10.1175/JAMC-D-14-0084.1.

IPCC, 2014: *Climate Change 2014: Synthesis Report. Contribution of Working Groups I, II and III to the Fifth Assessment Report of the Intergovernmental Panel on Climate Change*. IPCC, Geneva, Switzerland, 151 pp.

Kunkel, K. E., L. Ensor, M. Palecki, D. Easterling, D. Robinson, K. G. Hubbard, and K. Redmond, 2009: A new look at lake-effect snowfall trends in the laurentian great lakes using a temporally homogeneous data set. *Journal of Great Lakes Research*, **35 (1)**, 23–29, https://doi.org/https://doi.org/10.1016/j.jglr.2008.11.003.

Kunkel, K. E., N. E. Wescott, and D. A. R. Kristovich, 2002: Assessment of potential effects of climate change on heavy lake-effect snowstorms near lake erie. *Journal of Great Lakes Research*, **28 (4)**, 521–536, https://doi.org/https://doi.org/10.1016/S0380-1330(02)70603-5.

Letcher, T., and S. Steiger, 2010: Lake-effect lightning climatology of the great lakes. *National Weather Digest*, **34 (2)**, 157–168, URL http://nwafiles.nwas.org/digest/papers/2010/Vol34No2/Pg157-Letcher-Steiger.pdf.

Liu, C., and Coauthors, 2017: Continental-scale convection-permitting modeling of the current and future climate of north america. *Climate Dynamics*, **49 (1)**, 71–95, https://doi.org/10.1007/s00382-016-3327-9.

Magnuson, J. J., and Coauthors, 2000: Historical trends in lake and river ice cover in the northern hemisphere. *Science*, **289 (5485)**, 1743–1746, https://doi.org/10.1126/science.289.5485.1743.

Mason, L. A., C. M. Riseng, A. D. Gronewold, E. S. Rutherford, J. Wang, A. Clites, S. D. P. Smith, and P. B. McIntyre, 2016: Fine-scale spatial variation in ice cover and surface temperature trends across the surface of the laurentian great lakes. *Climatic Change*, **138 (1)**, 71–83, https://doi.org/10.1007/s10584-016-1721-2.

Minder, J. R., T. W. Letcher, L. S. Campbell, P. G. Veals, and W. J. Steenburgh, 2015: The evolution of lake-effect convection during landfall and orographic uplift as observed by profiling radars. *Monthly Weather Review*, **143 (11)**, 4422–4442, https://doi.org/10.1175/MWR-D-15-0117.1.

Moore, P. K., and R. E. Orville, 1990: Lightning characteristics in lake-effect thunderstorms. *Monthly Weather Review*, **118 (9)**, 1767–1782, https://doi.org/10.1175/1520-0493(1990)118⟨1767:LCILET⟩2.0.CO;2.

National Weather Service, 2006: Lake effect snow event archive: October 12, 2006 to october 13, 2006. Tech. rep., National Weather Service Weather Forecast Office Buffalo NY. URL https://www.weather.gov/buf/lesEventArchive2006-2007_a.

National Weather Service, 2014a: Lake effect summary: November 17-19, 2014. Tech. rep., National Weather Service Weather Forecast Office Buffalo NY. URL https://www.weather.gov/buf/lake1415_stormb.html.

National Weather Service, 2014b: Lake effect summary: November 19-21, 2014. Tech. rep., National Weather Service Weather Forecast Office Buffalo NY. URL https://www.weather.gov/buf/lake1415_stormc.html.

National Weather Service, 2022: Lake effect summary: December 23-27, 2022. Tech. rep., National Weather Service Weather Forecast Office Buffalo NY. URL https://www.weather.gov/buf/lesEventArchive?season=2022-2023&event=D.

Niziol, T. A., 1987: Operational forecasting of lake effect snowfall in western and central new york. *Weather and Forecasting*, **2 (4)**, 310–321, https://doi.org/10.1175/1520-0434(1987)002⟨0310:OFOLES⟩2.0.CO;2.

Niziol, T. A., W. R. Snyder, and J. S. Waldstreicher, 1995: Winter weather forecasting throughout the eastern united states. part iv: Lake effect snow. *Weather and Forecasting*, **10 (1)**, 61–77, https://doi.org/10.1175/1520-0434(1995)010⟨0061:WWFTTE⟩2.0.CO;2.

Northeast Regional Climate Center, 2025: Season-to-date regional snowfall departures, URL https://www.nrcc.cornell.edu/regional/monthly/monthly.html, accessed May 27th, 2025.

Notaro, M., V. Bennington, and S. Vavrus, 2015: Dynamically downscaled projections of lake-effect snow in the great lakes basin. *Journal of Climate*, **28 (4)**, 1661–1684, https://doi.org/10.1175/JCLI-D-14-00467.1.

Passarelli, R. E., and R. R. Braham, 1981: The role of the winter land breeze in the formation of great lake snow storms. *Bulletin of the American Meteorological Society*, **62 (4)**, 482–491, https://doi.org/10.1175/1520-0477(1981)062⟨0482:TROTWL⟩2.0.CO;2.

Rasmussen, R., and Coauthors, 2011: High-resolution coupled climate runoff simulations of seasonal snowfall over colorado: A process study of current and warmer climate. *Journal of Climate*, **24 (12)**, 3015–3048, https://doi.org/10.1175/2010JCLI3985.1.

Reinking, R. F., and Coauthors, 1993: The lake ontario winter storms (lows) project. *Bulletin of the American Meteorological Society*, **74 (10)**, 1828–1850, https://doi.org/10.1175/1520-0477-74-10-1828.

Schär, C., C. Frei, D. Lüthi, and H. C. Davies, 1996: Surrogate climate-change scenarios for regional climate models. *Geophysical Research Letters*, **23 (6)**, 669–672, https://doi.org/https://doi.org/10.1029/96GL00265.

Steiger, S. M., R. Hamilton, J. Keeler, and R. E. Orville, 2009: Lake-effect thunderstorms in the lower great lakes. *Journal of Applied Meteorology and Climatology*, **48 (5)**, 889–902, https://doi.org/10.1175/2008JAMC1935.1.

Steiger, S. M., T. Kranz, and T. W. Letcher, 2018: Thunderstorm characteristics during the ontario winter lake-effect systems project. *Journal of Applied Meteorology and Climatology*, **57 (4)**, 853–874, https://doi.org/10.1175/JAMC-D-17-0188.1.

Steiger, S. M., and Coauthors, 2013: Circulations, bounded weak echo regions, and horizontal vortices observed within long-lake-axis-parallel–lake-effect storms by the doppler on wheels. *Monthly Weather Review*, **141 (8)**, 2821–2840, https://doi.org/10.1175/MWR-D-12-00226.1.

Steiger, S. M., and Coauthors, 2024: Winter lightning to the lee of lake ontario: The lake-effect electrification (lee) field campaign. *Bulletin of the American Meteorological Society*, **105 (11)**, E2026–E2046, https://doi.org/10.1175/BAMS-D-23-0176.1.

Suriano, Z. J., 2019: Changing intrasynoptic type characteristics and interannual frequencies of circulation patterns conducive to lake-effect snowfall. *Journal of Applied Meteorology and Climatology*, **58 (10)**, 2313–2328, https://doi.org/10.1175/JAMC-D-19-0069.1.

Suriano, Z. J., and D. J. Leathers, 2017: Synoptic climatology of lake-effect snowfall conditions in the eastern great lakes region. *International Journal of Climatology*, **37 (12)**, 4377–4389, https://doi.org/https://doi.org/10.1002/joc.5093.

Vavrus, S., M. Notaro, and A. Zarrin, 2013: The role of ice cover in heavy lake-effect snowstorms over the great lakes basin as simulated by regcm4. *Monthly Weather Review*, **141 (1)**, 148–165, https://doi.org/10.1175/MWR-D-12-00107.1.

Wang, J., X. Bai, H. Hu, A. Clites, M. Colton, and B. Lofgren, 2012: Temporal and spatial variability of great lakes ice cover, 1973–2010. *Journal of Climate*, **25 (4)**, 1318–1329, https://doi.org/10.1175/2011JCLI4066.1.

Wright, D. M., D. J. Posselt, and A. L. Steiner, 2013: Sensitivity of lake-effect snowfall to lake ice cover and temperature in the great lakes region. *Monthly Weather Review*, **141 (2)**, 670–689, https://doi.org/10.1175/MWR-D-12-00038.1.